Reply to Referee #1

General comments:

This manuscript reports high-resolution measurements of net community production in the coastal South China Sea in summer and fall, as estimated using the dissolved O_2/Ar technique. The authors compare measured NCP rates against physical parameters and nutrient concentrations to assess factors influencing the spatial distribution and magnitude of productivity. These new NCP data are a useful contribution in that productivity measurements in this region to date have remained relatively sparse and low-resolution, but apart from presenting this new data the manuscript offers few broader or novel conclusions and the wider scientific significance is limited.

The field, experimental, and statistical analyses appear to have been rigorously conducted largely according to current best practices. In particular the methods indicate a good experimental setup and attention to potential sources of error in field O_2/Ar measurements.

In some cases, however, the conclusions regarding the influence of light and nutrients upon productivity patterns that the authors draw from their data and results are not fully appropriate or justified.

The presentation of data in the manuscript and figures is generally good, but leaves some room for improvement. The text could have benefited from better description of some data and variables, while Figure 1 is difficult to interpret, in turn impacting interpretation of other figures and results throughout the paper.

The major point this reviewer would like to stress is that the authors should pay careful attention to qualifying the caveats to some conclusions, while reconsidering other conclusions if they are not fully backed by the presented analyses.

Response: Thank you very much for your constructive comments. We have considered all suggestions and incorporated them into the revised version. In the following we answer to your comments point by point and indicate how the manuscript is going to be revised.

1. The conclusion that NCP is subject to nitrogen limitation based on correspondences between elevated NCP rates and DIN concentrations needs further justification. Nutrient concentrations reflect the marine environment at the moment of sampling, while the O_2/Ar method integrates over the residence time of biological oxygen in the surface ocean. The residence time is a particularly important factor for the authors to highlight in the manuscript, as it carries important implications for how far temporally removed the measured productivity signal is relative to the cruise measurements. At a minimum, additional discussion of the residence time of the oxygen signal on both cruises and potential associated considerations is necessary. Given the availability of satellite data as presented in He et al., 2016, discussion of the history of the measured water masses should be quite feasible. The reviewer also notes that the nitrogen limitation in this region is hardly a novel finding, as the authors themselves mention in the introduction. Mixed layer depth ranges and O_2 surface layer residence time should be directly reported in the text of the results.

Response: Thanks for your suggestion. We have reported the residence time of O_2 in the mixed layer in both cruises together with other parameters such as mixed layer depth and euphotic depth by adding two tables (Table 1 and 2), and incorporated them into the results and discussion. We have also applied the satellite-Chl a data (https://resources.marine.copernicus.eu) to track the history of shelf water intrusion and combined it with the residence time of O_2 to strengthen the reliability of the relationship between NCP and nitrogen we observed. Table 3 and Figure S3 were added in the new version accordingly. Δday in Table 3 is the difference between the date of observation and the start date of shelf water intrusion at stations with surface salinity lower than 33, representing the duration of the shelf water intrusion at each station before our observation. The mixed layer O_2 residence time at most stations listed in Table 3 is shorter than or equivalent to Δday. This result suggests that our estimate has appropriately integrated the NCP during the period of shelf water intrusion, which can effectively reflect the influence of shelf water on productive state on the northern slope of SCS in the summer.

The nitrogen limitation in SCS has been reported before, but so far no research has focused on quantifying the NCP enhancement caused by shelf water intrusion in this region. Our research is also the first report that quantifies the contribution of shelf water intrusion to NCP on the northern slope of the SCS in the summer. We have highlighted this in the introduction and conclusion section.

Table 1. Basic information at all CTD stations in October 2014

Station	Date of observation[a]	MLD (m)	Z_{eu}[b] (m)	k[c] (m d^{-1})	τ[d] (d)
O-01	2014/10/13	58	82	4.7	12
O-02	2014/10/13	64	74	5.2	12
O-03	2014/10/14	56	84	6.2	9
O-04	2014/10/14	54	76	6.3	9
O-05	2014/10/20	27	70	7.9	3
O-06	2014/10/19	55	62	8.4	7
O-07	2014/10/21	40	60	7.3	5
O-08	2014/10/21	49	72	7.4	7
O-09	2014/10/15	79	96	6.2	13
O-10	2014/10/15	68	81	6.1	11
O-11	2014/10/15	64	81	5.4	12
O-12	2014/10/16	66	74	5.2	13
O-13	2014/10/16	48	52	6.3	8
O-14	2014/10/17	54	62	6.9	8
O-15	2014/10/22	49	68	7.0	7
O-16	2014/10/22	50	73	7.3	7
O-17	2014/10/23	52	75	7.9	7
O-19	2014/10/18	31	64	9.4	3
O-20	2014/10/18	35	61	8.7	4
O-21	2014/10/18	81	86	6.9	12
O-22	2014/10/17	76	102	6.0	13

[a] All dates are in the format of year/month/day. [b] Euphotic depth, defined based on subsurface chlorophyll maximum layer. [c] Gas transfer velocity of O_2. [d] Residence time of O_2 in the mixed layer, estimated as per MLD/k.

Table 2. Basic information at all CTD stations in June 2015

Station	Date of observation	MLD (m)	Z_{eu} (m)	k (m d^{-1})	τ (d)
J-01	2015/6/18	26	63	2.2	12
J-02	2015/6/17	19	80	1.9	10
J-03	2015/6/16	20	74	1.9	11
J-04	2015/6/15	22	74	1.9	11
J-05	2015/6/15	11	78	1.2	9
J-06	2015/6/14	24	76	2.1	11
J-07	2015/6/13	21	81	2.3	9
J-08	2015/6/18	14	56	1.7	8
J-09	2015/6/19	17	59	1.6	10
J-10	2015/6/19	8	46	1.4	6
J-11	2015/6/20	8	40	2.8	3
J-12	2015/6/21	16	45	3.0	5
J-13	2015/6/21	19	45	2.3	8
J-14	2015/6/24	28	55	4.0	7
J-15	2015/6/24	17	42	5.3	3
J-16	2015/6/25	10	19	5.7	2

Table 3. The start date and duration (Δday) of shelf water intrusion at stations with surface salinity lower than 33 in June 2015

Station	Date of observation	Start date of shelf water intrusion	Δday[a]	τ (d)
J-09	2015/6/19	2015/6/10	9	10
J-10	2015/6/19	2015/6/13	6	6
J-11	2015/6/20	2015/6/13	7	3
J-12	2015/6/21	2015/6/13	8	5
J-13	2015/6/21	2015/6/13	8	8
J-16	2015/6/25	before 2015/6/10	> 15	2

[a] The difference between the date of observation and the start date of shelf water intrusion at listed stations.

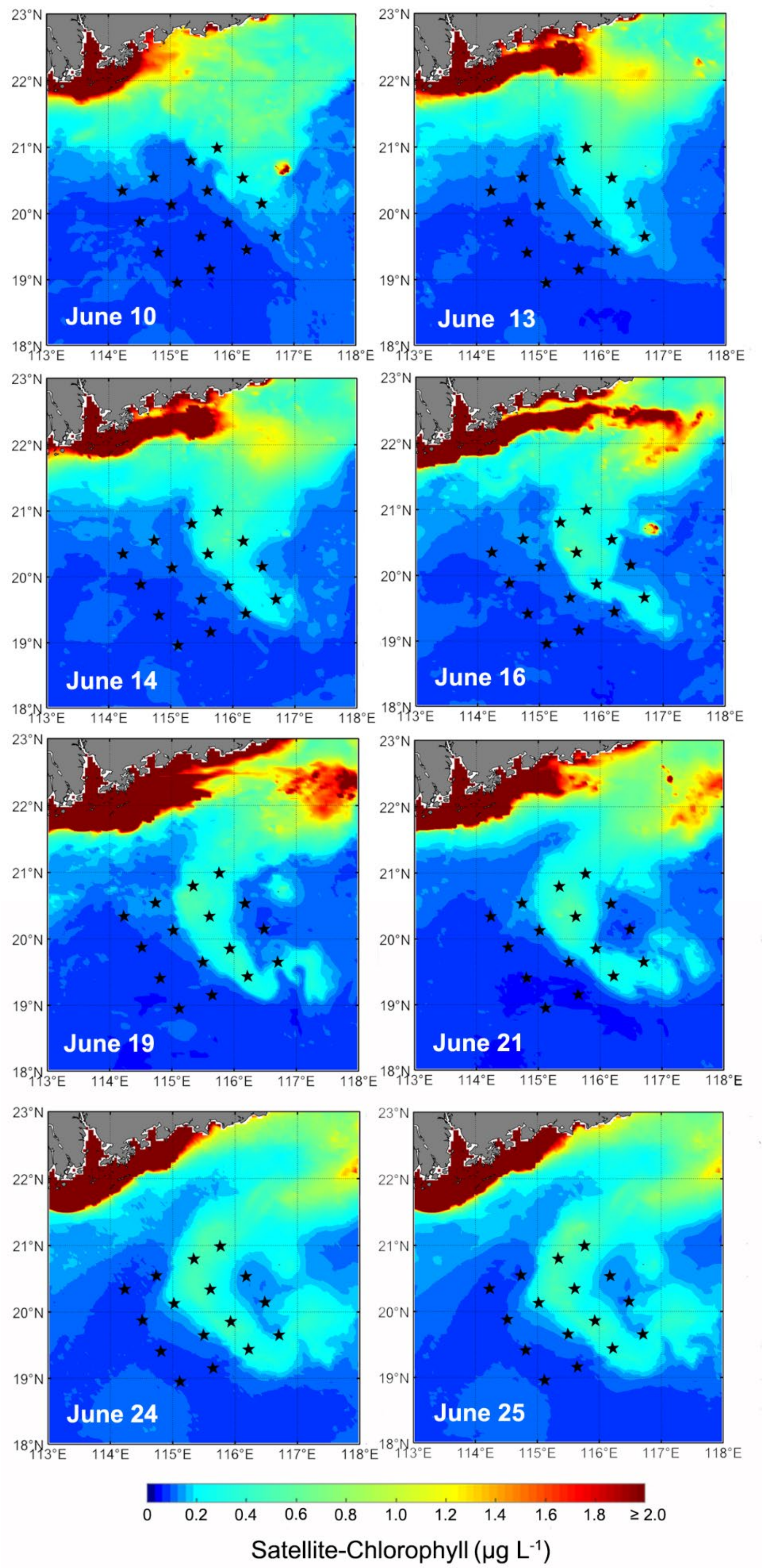

Figure S3. Daily satellite-chlorophyll on selected date from June 10 to 25, 2015. Stars represent CTD locations. We roughly set light blue (represents ~ 0.2 μg L^{-1}) in this figure as the criterion of shelf water

2. Similarly, assertions regarding the influence of light availability on NCP are questionable. Are MLDs around the time of these cruises really deep enough for light to influence mixed-layer productivity? In June of 2015 the data indicate that the maximum MLD value was just 30m. Water column PAR and Chl profiles are undoubtedly available from the CTD casts and should be presented and discussed in the context of such claims. A June 2015 Chl-a maxima of 0.6 ug/L certainly suggests that biomass-induced light attenuation in the mixed layer wouldn't be an issue, etc: : : Furthermore, residence time should once again be discussed, as light limitation is a factor influencing the time integrated productivity signal over the relevant wind speed history at the measurement sites. Figure 10 also seems to suggest that the strength of MLD relationships with NCP are dependent on a relatively low number of data points.

Response: Thanks for your suggestion. Because of your comment and the comments of reviewer 2, we have noticed the limitation of our analysis of MLD and NCP_{vol}. The negative correlation between NCP_{vol} and MLD we obtained may partly result from that NCP_{vol} is calculated by NCP/MLD. Thus we calculate an average surface PAR by integrating the daily satellite-PAR data obtained from NASA's ocean color website (https://oceancolor.gsfc.nasa.gov/l3) over the residence time of O_2 at each selected station in October 2014. 8-day PAR data were used to estimate the missing daily data. Then we use light attenuation coefficient (K_d) to calculate an average PAR in the mixed layer to make a correlation analysis with NCP. This new analysis gives a result that light availability is not a limitation on NCP in the SCS (Table 4), much more convincing than the former analysis just based on MLD.

The calculation of K_d basically based on Lambert-Beer law (Kirk 1994; Jerlov 1976):

$$K_d = -\frac{1}{z}\ln\frac{E_d(z)}{E_d(0)} = \frac{4.605}{Z_{eu}}$$

Where K_d (m^{-1}) is the light attenuation coefficient in the euphotic layer; $E_d(0)$ is the PAR at the surface, integrating an average over the residence time of O_2 before our observation, in the unit of mol m^{-2} d^{-1}; z represents a depth (m) and $E_d(z)$ is the PAR at this depth; Z_{eu} is the euphotic depth (m).

References: Kirk, J. T.: Light and photosynthesis in aquatic ecosystems, Cambridge university press, UK, 1994.
Jerlov, N. G.: Marine optics, Elsevier, Netherlands, 1976.

Table 4. Satellite-PAR data and NCP at selected stations in October 2014

Station	Date of observation	MLD (m)	Z_{eu} (m)	Surface PAR[a] (mol m^{-2} d^{-1})	K_d (m^{-1})	ML PAR[b] (mol m^{-2} d^{-1})	NCP (mmol C m^{-2} d^{-1})
O-01	2014/10/13	58	82	42.0	$5.6 * 10^{-2}$	12.0	3.0
O-02	2014/10/13	64	74	42.0	$6.2 * 10^{-2}$	10.0	15.1
O-03	2014/10/14	56	84	41.1	$5.5 * 10^{-2}$	12.4	10.1
O-08	2014/10/21	49	72	38.7	$6.4 * 10^{-2}$	11.4	15.7
O-10	2014/10/15	68	81	40.0	$5.7 * 10^{-2}$	9.8	4.4
O-13	2014/10/16	48	52	39.2	$8.9 * 10^{-2}$	8.7	15.3
O-15	2014/10/22	49	68	38.6	$6.8 * 10^{-2}$	10.8	16.3
O-20	2014/10/18	35	61	39.2	$7.5 * 10^{-2}$	13.3	16.4
O-22	2014/10/17	76	102	42.2	$4.5 * 10^{-2}$	11.6	15.7

[a] Average surface PAR over the residence time of O_2 in the mixed layer. [b] Average PAR in the mixed layer.

3. The claim at lines 426-428 that "there was no significant productivity below the mixed layer that was missed by underway sampling" also seems unjustified and contradicts earlier results and text. Earlier for instance, the authors note that a subsurface oxygen maximum is a characteristic feature in the South China Sea, and significant subsurface productivity is observed in many oligotrophic regions globally such as the Sargasso Sea. Vertical Chl profiles would again be important evidence to present in support of the claim that underway measurements did not miss significant subsurface production.

Response: Sorry for this arbitrary conclusion. We have deleted it. Subsurface chlorophyll maximum layer (SCML) existed at all stations in both cruises, while the obvious subsurface O_2 maximum just existed in Transect 1 and 2 in June 2015. We have reported these results in section 3.2. Both SCML and subsurface O_2 maximum were below the MLD, indicating that they might not influence the NCP in the mixed layer a lot.

4. In general, since Delta O_2/Ar is directly used to calculate NCP, reporting and discussing relationships between Delta O_2/Ar and other parameters provides little value. This reviewer would recommend removing discussions of Delta O_2/Ar versus Chl, MLD, and so on from the manuscript.

Response: Thanks for your suggestion. We have done that and also removed related figures from Figure 8 and 9.

5. The authors should also consider whether alternative hypotheses (nutrient co-limitation, limitation by a non-measured variable such as Fe, etc: : :) could potentially present alternative explanations for observed patterns/relationships.

Response: Thanks for your suggestion. We had tried to analyze the relationships between NCP and Fe, N:P ratio, but we didn't find any valuable result to report. Zhang et al. (2019) reported that Fe may not be a limitation to phytoplankton growth on the northern slope of SCS. In addition, we didn't find significant correlation between Fe (data provided by Ruifeng Zhang) and NCP in the mixed layer in Oct. 2014, thus we didn't report this result. N is acknowledged as the major limitation of primary production in the SCS, and P deficiency usually occurs when excessive river runoff results in a high N:P ratio nutritive state (Lee Chen and Chen 2006). N:P ratio is an important basis for judging whether the main influencing factor on NCP is N or P in the SCS. But most of our nutrients data in the mixed layer are too low to support a convincing analysis of N:P ratio. We have added some background information of these alternative hypotheses in the introduction section.

References: Zhang, R., Zhu, X., Yang, C., Ye, L., Zhang, G., Ren, J., Wu, Y., Liu, S., Zhang, J. and Zhou, M.: Distribution of dissolved iron in the Pearl River (Zhujiang) Estuary and the northern continental slope of the South China Sea, Deep. Res. Part II Top. Stud. Oceanogr., 167, 14–24, doi:10.1016/j.dsr2.2018.12.006, 2019.

Lee Chen, Y. and Chen, H.: Seasonal dynamics of primary and new production in the northern South China Sea: The significance of river discharge and nutrient advection, Deep Sea Res. Part I Oceanogr. Res. Pap., 53(6), 971–986, doi:10.1016/j.dsr.2006.02.005, 2006.)

Specific comments:

Lines 13-14: it should be clarified at the very start of the abstract that the O_2/Ar ratio refers to dissolved gases in surface seawater.

Response: Following your suggestion, we started the abstract with *"Dissolved oxygen-to-argon ratios (O_2/Ar) in the oceanic mixed layer has been widely used to estimate net community production (NCP), which is the difference between gross primary production and community respiration and is a proxy of carbon export from the surface ocean."*.

Line 32: Rather than oceanic CO_2 uptake, which is strongly dominated by physical factors, it might be more appropriate to say that oceanic carbon sequestration is regulated by primary production and export.

Response: Thanks for your suggestion. We have changed the oceanic CO_2 uptake to oceanic carbon sequestration.

Line 38: No longer recent: : : quite an established technique at this point.

Response: We agree with the reviewer that using the O_2/Ar ratio to estimate NCP is an established technique, hence the word 'Recently' was deleted.

Line 41: No longer clear that coastal O_2/Ar-derived estimates of NCP are sparse.

Response: Thanks for your suggestion. We have revised this paragraph and it now reads as *"During recent years, several high-resolution measurements of O_2/Ar and NCP in coastal waters have been reported (Tortell et al., 2012; Tortell et al., 2014; Eveleth et al., 2017; Izett et al., 2018). Despite the coastal waters such as shelves and estuaries only account for 7 % of the global ocean surface area, they are known to contribute to 15–30 % of the total oceanic primary production (Bi et al., 2013; Cai et al., 2011) and play an important role in marine carbon cycle and production. However, these regions still suffer from low resolution measurements and are poorly represented in global NCP data sets."*

Line 97: This is minor, but the original publication describing the MIMS technique (Tortell, L&O: Methods, 2005) should be cited here.

Response: Thanks for your suggestion. We have cited this paper here.

Line 158: Clarify units.

Response: The unit here is $\mu g\ L^{-1}$.

Lines 170-175: For this section, units for density should be in kg/mˆ3 to arrive at the correct units for NCP, or the appropriate conversion factor

Response: We have revised it as suggested.

Line 181: remove "excellent"

Response: We have deleted it.

Lines 213-220: Encourage authors to also display the ranges for SSS and Chl-a for the June 2015 cruise using the same format employed in the paragraph above for the October 2014 cruise, for consistency and clarity.

Response: Thanks for your suggestion. We have done that as suggested.

Lines 225-227: Elaborating on the assertion that high O_2/Ar and low pCO_2 signify a strong biological CO_2 sink may be useful. The pCO_2 values are indeed considerably low and I would be curious about the associated residence time of O_2/Ar on Transect 3.

Response: Thanks for your suggestion. We have applied an atmospheric pCO_2 obtained in July 2015 in the SCS to calculate a $\triangle pCO_2$, directly showing the difference of pCO_2 between surface water and atmosphere. We have also cited related paper to clarify that the negative $\triangle pCO_2$ in Transect 3 represented a strong CO_2 sink (Li et al., 2020). It's arbitrary to say "biological CO_2 sink", because this strong sink might not be totally caused by biological process. Thus we delete "biological". Residence time of O_2 at all CTD stations has been shown in Table 1 and 2.

References: Li, Q., Guo, X., Zhai, W., Xu, Y. and Dai, M.: Partial pressure of CO_2 and air-sea CO_2 fluxes in the South China Sea: Synthesis of an 18-year dataset, Prog. Oceanogr., 182, doi:10.1016/j.pocean.2020.102272, 2020.

Line 236 and elsewhere: Here and throughout the paper, you are reporting averages as ##.## +/- ##.##. You should specify that these represent avg +/- std dev: : : etc: : :

Response: Thanks for your suggestion. We have clarified this in the first paragraph of Results and Discussion： *"In addition, please note that all averages we have published in this paper are reported in the format of mean ± standard deviation".*

Lines 299-301: Keep it clear in this sentence that upwelling does not necessarily produce an underestimation of NCP. It is more accurate to say that subsurface waters may have different (either more positive or more negative) O_2/Ar signatures that could produce either an underestimation or an underestimation of NCP, as you explain a few sentences later in the context of subsurface O_2 maxima in oligotrophic regions.

Response: Thanks for your suggestion. We have revised the sentences as "*Vertical mixing is considered the largest source of error in O_2/Ar-based NCP estimates because the upwelled subsurface water with different O_2/Ar signatures can produce either an overestimation or an underestimation of NCP in the mixed layer (Cassar et al., 2014; Izett et al., 2018). Former researches usually ignored the underestimated negative NCP that caused by vertical mixing (Giesbrecht et al., 2012; Reuer et al., 2007; Stanley et al., 2010).*"

Lines 313-315: The cutoff for salinity to account for waters influenced by shelf water injection is justified, but the cutoff intended to exclude regions with upwelling seems somewhat arbitrary.

Response: Sorry for that. We have specified the criteria of upwelling as "*the regions with negative NCP and the regions with salinity higher than 33.5 and temperature lower than 30 °C in Transect 4*". There are lots of overlap of these two criteria, effectively removing the upwelling regions.

Line 330: Consideration of other explanations is needed in this section as described in the general comments.

Response: Thanks for your suggestion. We have reported the residence time of O_2 and related it to the history of shelf water intrusion based on daily satellite-chl a data in the revised manuscript. Please see our reply to comments 1 for more detail.

Lines 412-418: As mentioned in the general comments, is it even meaningful to analyze the influence of light limitation on NCP when the euphotic zone is 2-7 times the depth of the mixed layer in this region? Much more discussion is needed to back this light limitation idea. Cassar et al 2011 makes the point for instance that MLD is not the only factor affecting light availability.

Response: Thanks for your suggestion. Because of your comment and the comments of reviewer 2, we have noticed the limitation of our analysis between MLD and NCP_{vol}. Cassar et al. (2011) pointed out that the correlation analysis between MLD and NCP actually reflected an iron-light co-limitation. Thus we decide not to use MLD as an indicator of light availability. In the revised manuscript, we calculate an average surface PAR by integrating the daily satellite-PAR data over the residence time of O_2 at each selected station in October 2014. Then we use light attenuation coefficient to calculate an average PAR in the mixed layer to make correlation analysis with NCP. Table 4 was added accordingly to show the results.

Lines 426-428: “This result implied that there was no significant productivity below the mixed layer that was missed by underway sampling.” As mentioned in the general comments, you need to address the contradiction between this and subsurface O_2 maxima and potential deep chlorophyll maxima.

Response: Sorry for this arbitrary conclusion. We have deleted it. Subsurface chlorophyll maximum layer (SCML) existed at all stations in both cruises, while the obvious subsurface O_2 maxima just existed at Transect 1 and 2 in June 2015. We have reported these results in section 3.2. Both SCML and subsurface O_2 maxima were below the MLD, indicating that they might not influence the mixed layer NCP a lot in the region without vertical mixing.

Figure 1, lines 681 - 683: please describe what the point and star symbols represent.
Are these the locations of CTD casts? The fact that the color scale in (a) and (b) represents bathymetry should also be stated as well. The cruise path in (a) is also difficult to interpret based on the arrows. This figure is critical for the interpretation of subsequent figures. Perhaps numbering of points on the cruise plan would convey the path of travel better.

Response: Thanks for your suggestion. Following your suggestion, we redraw this figure and added an explanation of the symbols and color scales to the caption. Two insets have been added in Figure 1a and 1b to show the station numbers better.

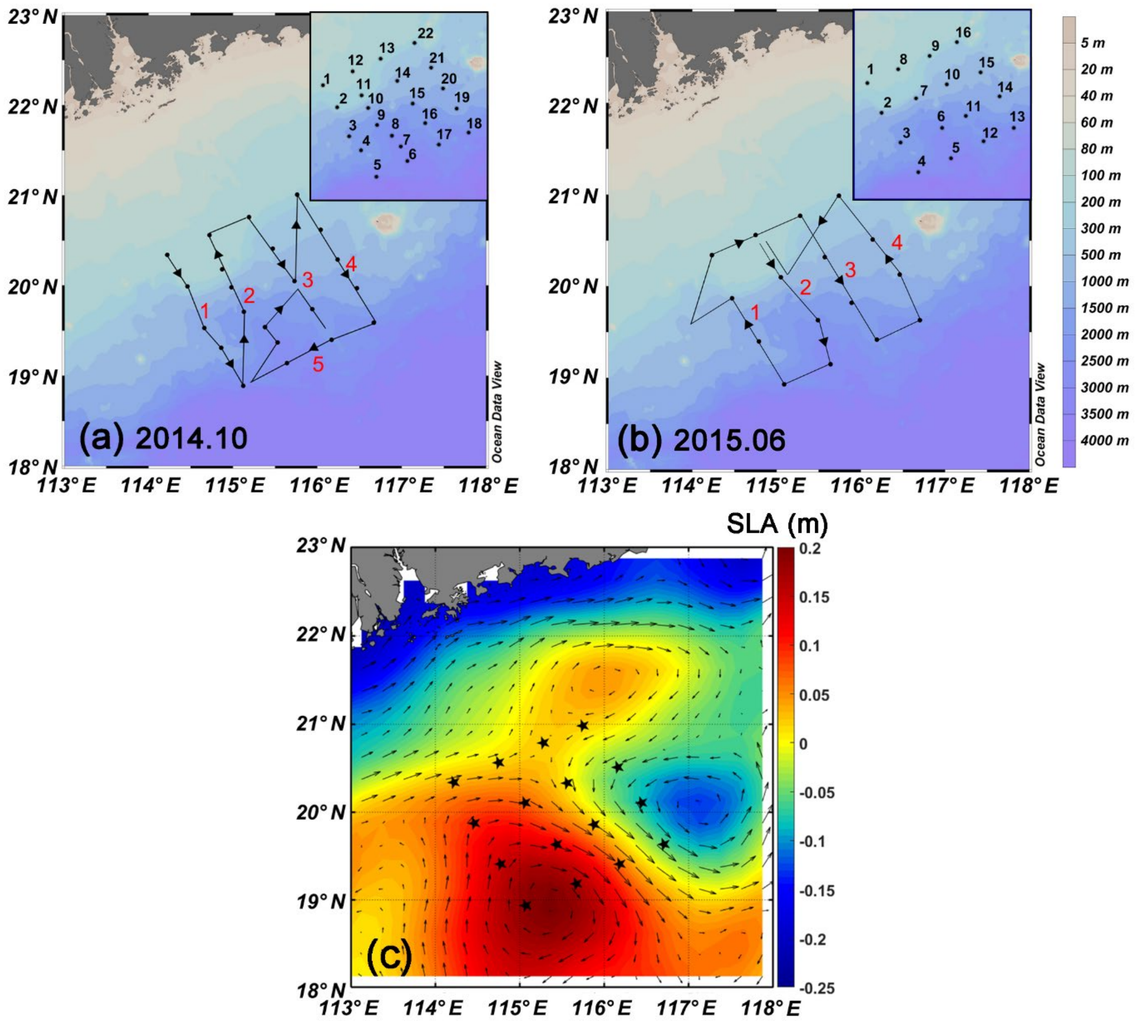

Figure 1. Cruise tracks of two cruises in the slope region of the Northern South China Sea in **(a)** October 2014, **(b)** June 2015. The sea level height anomaly (SLA) and geostrophic current during observations in June 2015 (Chen et al., 2016) are shown in **(c)**. The black dots/stars represent the locations of the CTD casts. Red numbers indicate transects, while black numbers indicate the serial number of CTD stations based on the cruise plan. The color scale in **(a)** and **(b)** represents bathymetry.

Technical corrections:

Lines 310-318: Here and elsewhere throughout the manuscript, you use sentence structures that rely too heavily on parentheses, which can cause confusion for readers.These sentences in particular are very difficult to interpret.

General: There are some grammatical errors in the conclusion

Response: We have reduced the number of parentheses in the text and revised the grammatical errors in the conclusion.

Reply to Referee #2

Thank you very much for your constructive comments. In the following we answer to your comments point by point and indicate how the manuscript is going to be revised.

General comments

In their manuscript "High-resolution distributions of O_2/Ar on the northern slope of the South China Sea and estimates of net community production", the authors report continuous net community production (NCP) estimates in the mixed layer of the northern South China Sea (SCS). The study makes a clear contribution to understanding of productivity in marginal seas like the SCS, where prior NCP estimates are limited. To a lesser extent, the study also advances a relatively novel method to estimating NCP through continuous observations of ΔO_2/Ar. My major critique is that the authors do not connect back to these original objectives in their paper. What new information have they gathered about the SCS as a result of this continuous method of measuring NCP, and how does this relate to past measurements of NCP in this region? Which methodological and/or environmental factors cause their estimates to compare or differ from past estimates? It is clear why their study is significant, but explicitly tying the discussion of results to these objectives will strengthen the scientific contributions of this paper.

Response: Following your suggestion, we amended the manuscript and described the importance of shelf water intrusion in the study region from line 84 to 88 that *"The northern slope of SCS is an important transition region between coastal area and SCS basin. In the summer, the shelf water intrusion is an important process changing the nutritive state in the northern slope region of SCS (He et al., 2016; Lee Chen and Chen, 2006). But so far, the NCP enhancement caused by this process is still unknown."* Besides to figure out the regulating factor on NCP, we also set quantifying the contribution of shelf water to the NCP enhancement in the study region as one of our main objectives. This can be a new finding achieved by our O_2/Ar method.

By comparing our NCP result with previous results, we emphasized the important influence of shelf water intrusion in the summer. In addition, we highlighted that our high-resolution observation can catch the rapid NCP variation more effectively than previous methods. Related content can be found in section 3.3 and 3.4 (lines 346 to 354, lines 409 to 417).

In the revised conclusion section, we pointed out that nitrogen is the main regulating factor on NCP in the study region and reported that *"the summer shelf water intrusion may significantly promote NCP by 376 %"*, connecting back to our objectives.

Specific comments

In the title: It is more accurate to write ΔO_2/Ar rather than O_2/Ar?

Response: We have changed O_2/Ar to $\Delta(O_2/Ar)$

Line 35: Clarify what "indicator" means in this context, and in which conditions this assumption holds true (e.g., NCP may be partitioned into DOC production, particle export, zooplankton grazing, etc.).

Response: NCP here represents the net organic carbon production in the mixed layer, corresponding to the difference of phytoplankton photosynthesis and respiration. Thus we can use the mass balance of biological O_2 to quantify NCP. NCP can be regarded as a sum of biological POC, DOC and the organic carbon involved in the food wed. O_2/Ar-based NCP used to rely on the steady state assumption that the productive rate and wind speed keep constant. We have incorporated these into the revised manuscript from line 39 to 44 that *"Net community production (NCP) corresponds to gross primary production (GPP) minus community respiration (CR) in the water (Lockwood et al.,* *2012; Stanley et al., 2010) and is an important indicator of carbon export. At steady state, NCP is equivalent to the rate of organic carbon export and transfer up the food web, which can quantify the strength of biological pump (Lockwood et al., 2012).*"

But recent researches pointed out that the O_2/Ar-based NCP estimate could be a time-weighted NCP over the residence time of O_2, weakening the need for the steady state assumption. We have clarified this in section 2.2.

Line 55: The water classifications are a bit confusing here. Perhaps it would be clearer to say that SCS water is a mix between two end-members: freshwater runoff from rivers and North Pacific offshore water.

Response: Sorry for the confusion caused. The SCS water is not just a mix between freshwater runoff and North Pacific offshore water. Because of its long residence time in the SCS region, its property has been changed a lot by heat exchange, precipitation and mixing processes. Li et al. (2018) regarded the SCS water as one of the end-members of water masses on the northern slope region of SCS. We have revised the manuscript to make this classification clearer. Now this content reads *"The surface water masses on the northern slope of SCS can be categorized into three regimes: shelf water, offshore water (e.g., the intruded Kuroshio water), and the SCS water (Feng, 1999; Li et al., 2018). The shelf water is mixed with fresh water from rivers or coastal currents and thus usually has low salinity (S < 33) and low density (Uu and Brankart, 1997; Su and Yuan, 2005; Cheng et al., 2014). Both offshore water and SCS water originate from the Northern Pacific. Thus offshore water has similar hydrographic characteristics of high temperature and high salinity as the Northern Pacific water. But the SCS water has changed a lot in its hydrographic property because of the mixing processes, heat exchange and precipitation during its long residence time in the SCS (Feng et al., 1999; Li et al., 2018).*"

Reference: Li, D., Zhou, M., Zhang, Z., Zhong, Y., Zhu, Y., Yang, C., Xu, M., Xu, D. and Hu, Z.: Intrusions of Kuroshio and Shelf Waters on Northern Slope of South China Sea in Summer 2015, J. Ocean Univ. China, 17(3), 477–486, doi:10.1007/s11802-018-3384-2, 2018.

Lines 70-84: It is unclear what the aim of listing these numbers is? Do the authors wish to convey that NCP is variable across SCS studies? It would be useful to reference these numbers again in the discussion for comparison. In any case, when reporting NCP and export, use both O_2 and C units so that the numbers are comparable. The authors can perhaps apply the photosynthetic quotient used in the method to do this conversion to keep units consistent (line 174).

Line 79: Should the units here be sˆ-1 rather than aˆ-1?

Response: Here we want to report the previous researches about carbon export in the SCS. The POC just occupies a portion of NCP, and its value may not be very comparable with NCP. Hence we deleted the description about previous POC export and mainly focus on the previous NCP researches in the SCS in this paragraph. We have cited the previous NCP values to compare with our NCP results in this study. We have also converted the unit of all NCP values mentioned in the text to "mmol C m^{-2} d^{-1}".

Lines 85-86: Describe the potential inaccuracies of each discrete method so that it is clearer how this study benefits scientific understanding of the SCS.

Response: Thanks for your suggestion. We revised the manuscript to describe the potential inaccuracies and shortcomings of discrete methods in the following paragraph as that *"Discrete sampling suffers from low spatial resolution, and cannot adequately resolve variabilities caused by small-scale physical or biological processes in dynamic marine systems. In addition, each of the three methods for NCP estimate mentioned above has its limitation. DIC-based NCP estimate is not suitable for the coastal region, because instead of biological* *metabolism, the terrestrial runoff can be the strongest factor influencing the DIC in the coastal system (Mathis et al., 2011). The inavoidable difference between in situ circumstance and on deck incubation condition can introduce uncertainties to the NCP derived from light/dark bottle incubation (Grande et al., 1989). Though Argo profiling float partly gets rid of the limitation of discrete sampling, it's hard to control its movement in the study region. However, no high-resolution measurement of NCP has been reported for the SCS so far."*

Section 2.2: Explain how the 5-minute NCP values are scaled up to daily estimates.

Lines 179-183: As written, these two sentences imply that the authors do not know whether their NCP estimates represent daily or monthly signals. If they represent the latter, would this not defeat the purpose of the study, which is to resolve "highly dynamic environmental fluctuations of coastal systems" (line 87) in shorter than monthly time scales?

Response: The "5-min" here is not a timescale for monitoring the net change of a biological production tracer during this period to calculate the daily NCP, but the time interval of our underway data. The 5-min interval is usually along with a spatial interval of 500 m to 1 km because the ship is moving, thus it can also be regarded as the spatial resolution of underway sampling, which is much higher than that of discrete sampling (e.g., CTD cast).

The "over the past month" used in the previous version is not very accurate, and we have revised it to "*during the residence time of oxygen in the mixed layer*". The $\Delta(O_2/Ar)$ we obtained is a cumulative result that had been influenced by the physical (e.g., air-sea exchange, water mixing) and biological processes (e.g., respiration and photosynthesis) during the residence time of oxygen in the mixed layer. The influence of "environmental fluctuations" during that period could be reflected by the physical and biological processes mentioned above, which certainly had a contribution to the final NCP values we estimated. That's why we can catch the dramatic high NCP and negative NCP resulted from shelf water intrusion and upwelling respectively in the June cruise.

Here we have intended to clarify that our NCP estimate is a time-weighted result instead of a daily average result. If the environment is at the steady state (e.g., constant productive rate and constant wind), our estimate can be an actual daily NCP. But in reality, steady state is always violated because of the variable wind-speed (or gas transfer velocity) over time. We apply a time-weighted scheme to calculate the gas transfer velocity following Reuer et al.(2007) and Teeter et al.(2018), more heavily weighting recent periods and storm periods to erase the importance of earlier states. As a result, though our NCP result is in the unit of $mmol\ C\ m^{-2}\ d^{-1}$, it's not the actual daily NCP but represents an estimate of time-weighted sea-to-air biological oxygen flux over the residence time of oxygen before our observation of O_2/Ar.

Reference: Reuer, M. K., Barnett, B. A., Bender, M. L., Falkowski, P. G. and Hendricks, M. B.: New estimates of Southern Ocean biological production rates from O_2/Ar ratios and the triple isotope composition of O_2, Deep Sea Res. Part I Oceanogr. Res. Pap., 54(6), 951–974, doi:10.1016/j.dsr.2007.02.007, 2007.

Teeter, L., Hamme, R. C., Ianson, D. and Bianucci, L.: Accurate Estimation of Net Community Production From O_2/Ar Measurements, Global Biogeochem. Cycles, 32(8), 1163–1181, doi:10.1029/2017GB005874, 2018.

Lines 412-416: Clarify how the DIN and NCP criteria were chosen for each cruise.

Fig. 10b is not very compelling as the lowest MLD - highest volumetric NCP data point seems to drive the negative correlation. Thus, the authors should consider removing their analysis of June 2015 data from Fig. 10b, and just discuss the analysis in the text in relation to the much stronger relationship between MLD and volumetric NCP during October 2014. Another related analysis that may be interesting is comparing NCP values at stations where MLD is deeper than the euphotic zone depth, to NCP at stations where the MLD is shallower than the euphotic zone depth.

Response: Thanks for your suggestion. The relationship shown in figure 10b is not convincing enough because of inadequate data points. In addition, during the June 2015 cruise, the euphotic zone was 2-7 times the depth of the mixed layer, thus it's not meaningful to discuss the light limitation in the summer. We selected 9 stations of October cruise where surface DIN concentration in the range of 0.10—0.17 μmol L^{-1} to make the analysis of NCP and light. Because of your comment and the comments of reviewer 1, we have noticed the limitation of our analysis between MLD and NCP_{vol}. The negative correlation between NCP_{vol} and MLD we obtained may partly result from that NCP_{vol} is calculated by NCP/MLD. Thus we calculate an average surface PAR by integrating the daily satellite-PAR data obtained from NASA ocean color website (https://oceancolor.gsfc.nasa.gov/l3) over the residence time of O_2 at each selected station in October 2014. 8-day PAR data were used to estimate the missing daily data. Then we use light attenuation coefficient (K_d) to calculate an average PAR in the mixed layer to make a correlation analysis with NCP. The results were shown in a new table (Table 4). This new analysis gives a result that light availability is not a limitation on NCP in the SCS, much more convincing than the former analysis just based on MLD.

The calculation of K_d basically based on Lambert-Beer law (Kirk 1994; Jerlov 1976):

$$K_d = -\frac{1}{z}\ln\frac{E_d(z)}{E_d(0)} = \frac{4.605}{Z_{eu}}$$

Where K_d (m^{-1}) is the light attenuation coefficient in the euphotic layer; $E_d(0)$ is the PAR at the surface, integrating an average over the residence time of O_2 before our observation, in the unit of mol m^{-2} d^{-1}; z represents a depth (m) and $E_d(z)$ is the PAR at this depth; Z_{eu} is the euphotic depth (m).

Table 4. Satellite-PAR data and NCP at selected stations in October 2014

Station	Date of observation	MLD (m)	Z_{eu} (m)	Surface PAR[a] (mol m^{-2} d^{-1})	K_d (m^{-1})	ML PAR[b] (mol m^{-2} d^{-1})	NCP (mmol C m^{-2} d^{-1})
O-01	2014/10/13	58	82	42.0	$5.6 * 10^{-2}$	12.0	3.0
O-02	2014/10/13	64	74	42.0	$6.2 * 10^{-2}$	10.0	15.1
O-03	2014/10/14	56	84	41.1	$5.5 * 10^{-2}$	12.4	10.1
O-08	2014/10/21	49	72	38.7	$6.4 * 10^{-2}$	11.4	15.7
O-10	2014/10/15	68	81	40.0	$5.7 * 10^{-2}$	9.8	4.4
O-13	2014/10/16	48	52	39.2	$8.9 * 10^{-2}$	8.7	15.3
O-15	2014/10/22	49	68	38.6	$6.8 * 10^{-2}$	10.8	16.3
O-20	2014/10/18	35	61	39.2	$7.5 * 10^{-2}$	13.3	16.4
O-22	2014/10/17	76	102	42.2	$4.5 * 10^{-2}$	11.6	15.7

[a] Average surface PAR over the residence time of O_2 in the mixed layer. [b] Average PAR in the mixed layer.

References: Kirk, J. T.: Light and photosynthesis in aquatic ecosystems, Cambridge university press, UK, 1994.

Jerlov, N. G.: Marine optics, Elsevier, Netherlands, 1976.

Technical comments

Figure 1: Explain what the dots/markers in the panels represent. Are they the locations of the CTD casts? If not, it is worth adding the locations of the CTD casts to this figure so that readers may better understand the interpolation of MLD between casts for underway data.

Response: Yes, the dots and stars are the locations of the CTD casts. Following your suggestion, we have added an explanation of these markers to the caption of figure 1, "*the black dots/stars represent the locations of the CTD casts*".

Figure 3: Why were there more variables in the June cruise? This is not clear in the methods.
Response: Sorry for that. During the cruise in October 2014, the DO sensor of RBR broke down, and we did not make the standards for CO_2 calibration. Thus there are no data of DO and pCO_2 in that cruise. We have clarified this in the section 2.1 which reads:
"We didn't obtain continuous DO data in October 2014 because the DO sensor of RBR broke down during this cruise."
"The instrumental CO_2 ion current was calibrated at about 12–24 h intervals using equilibrated seawater standards as per Guéguen and Tortell (2008) during the survey in June 2015."

Figure 5: Write in the salinity units. It is worth clarifying somewhere in the figure text, as well as the main text referencing Fig. 5, that the temperature fluctuations shown here are too small to reflect upwelling.
Figure 6: Write in the salinity units.
Figure 8: Write in the salinity units.
Figure 9: Write in the salinity units.
Response: Thanks for your suggestions. We have added the units of salinity on these figures as well as figure 2 & 3. We have also clarified in the main text that the temperature fluctuations shown in figure 5 are too small to reflect upwelling.

Figure S1: This actually is referenced after Fig. S2 so consider switching the figure order. Why is [NO_3^-] omitted here?
Response: Thanks for your suggestion. We have switched the order of figure S1 & S2. The surface NO_3^- concentration was below the detection limit at all sampling stations during the cruise in 2014, thus we didn't make the plot for [NO_3^-]. We had clarified this in the figure caption that *"The surface concentration of nitrate (NO_3^-) at all sampling stations was below the detection limit during this cruise."*.

Figures S3-S7: These are not referenced in the text, but they should be if they are to be published. Otherwise, it is not clear what the significance of showing these data are, as they could just go on an online repository which gets referenced in the text.
Response: Thanks for your suggestion. These transects are not very representative, so we didn't discuss them in the text. We decided to delete these figures from the supplementary. But the data of these transects can be easily downloaded from the online repository we shared.

High-resolution distributions of Δ(O_2/Ar) on the northern slope of the South China Sea and estimates of net community production

Chuan Qin[1,2], Guiling Zhang[1,2,*], Wenjing Zheng[1], Yu Han[1,3], Sumei Liu[1,2]

1. Key Laboratory of Marine Chemistry Theory and Technology, Ministry of Education/Institute for Advanced Ocean Study, Ocean University of China, 238 Songling Road, 266100 Qingdao, P. R. China
2. Laboratory for Marine Ecology and Environmental Science, Qingdao National Laboratory for Marine Science and Technology, Qingdao 266237, P. R. China
3. Hainan Tropical Ocean University, Sanya 572022, P. R. China

* Correspondence to: Guiling Zhang (guilingzhang@ouc.edu.cn)

Abstract

Dissolved oxygen-to-argon ratios (O_2/Ar) in the oceanic mixed layer has been widely used to estimate net community production (NCP), which is the difference between gross primary production and community respiration and is a proxy of carbon export from the surface ocean. In order to obtain the high-resolution distribution of NCP and improve our understanding of its regulating factors in the slope region of the Northern South China Sea (SCS), we conducted continuous measurements of dissolved O_2, Ar, and CO_2 by membrane inlet mass spectrometry during two cruises in October 2014 and June 2015. An overall autotrophic condition was observed in the study region in both cruises with an average Δ(O_2/Ar) of 1.1 % ± 0.9 % in October 2014 and 2.7 % ± 2.8 % in June 2015. NCP was on average 11.5 ± 8.7 mmol C m^{-2} d^{-1} in October 2014 and 11.6 ± 12.7 mmol C m^{-2} d^{-1} in June 2015. Correlations between dissolved inorganic nitrogen (DIN), Δ(O_2/Ar), and NCP were observed in both cruises, indicating that NCP is subject to the nitrogen limitation in the study region. In June 2015, we observed a rapid response of the ecosystem to the episodic nutrient supply induced by eddies. Eddy-entrained shelf water intrusion, which supplied large amounts of terrigenous nitrogen to the study region, promoted NCP in the study region by 376 %. In addition, upwelling brought large uncertainties to the estimation of NCP at the core region of the cold eddy (cyclone) in June 2015. The deep euphotic depth in the SCS and the absence of correlation between NCP and the average photosynthetically available radiation (PAR) in the mixed layer in the autumn indicate that light availability may not be a significant limitation on

NCP in the SCS. This study helps to understand the carbon cycling in the highly dynamic shelf system.

Keywords: O_2/Ar; Net community production; Nutrients; Eddy; Northern slope of South China Sea

1. Introduction

The oceanic carbon sequestration is partially regulated by the production and export process of biological organic carbon in the surface ocean. Net community production (NCP) corresponds to gross primary production (GPP) minus community respiration (CR) in the water (Lockwood et al., 2012) and is an important indicator of carbon export. At steady state, NCP is equivalent to the rate of organic carbon export and transfer up the food web, which can quantify the strength of biological pump (Lockwood et al., 2012). Dissolved oxygen-to-argon ratio (O_2/Ar) has been developed as a proxy for NCP in a water mass based on the similar physical properties of O_2 and Ar (Craig and Hayward, 1987; Kaiser et al., 2005). The biological production in the open oceans (i.e., Southern Ocean, Pacific, Arctic Ocean) has been inferred using the O_2/Ar ratio to estimate NCP in numerous researches (e.g., Hamme et al., 2012; Lockwood et al., 2012; Ulfsbo et al., 2014; Shadwick et al., 2015; Stanley et al., 2010). During recent years, several high-resolution measurements of O_2/Ar and NCP in coastal waters have been reported (Tortell et al., 2012; Tortell et al., 2014; Eveleth et al., 2017; Izett et al., 2018). Despite the coastal waters such as shelves and estuaries only account for 7 % of the global ocean surface area, they are known to contribute to 15–30 % of the total oceanic primary production (Bi et al., 2013; Cai et al., 2011) and play an important role in marine carbon cycle and production. However, these regions still suffer from low resolution measurements and are poorly represented in global NCP data sets.

The South China Sea (SCS) is one of the largest marginal seas in the world with extremely complex ecological characteristics. River runoff from the Pearl and Mekong Rivers introduces large amounts of dissolved nutrients into the SCS (Ning et

删除的内容: CO_2 uptake

删除的内容: Recently, t

al., 2004). Due to the influence of seasonal monsoons, the surface circulation in the SCS changes from a basin-scale cyclonic gyre in winter to an anticyclonic gyre in summer (Hu et al., 2000). The surface water masses on the northern slope of SCS can be categorized into three regimes: shelf water, offshore water (e.g., the intruded Kuroshio water), and the SCS water (Feng, 1999; Li et al., 2018). The shelf water is mixed with fresh water from rivers or coastal currents and thus usually has low salinity (S < 33) and low density (Uu and Brankart, 1997; Su and Yuan, 2005; Cheng et al., 2014). Both offshore water and SCS water originate from the Northern Pacific. Thus offshore water has similar hydrographic characteristics of high temperature and high salinity as the Northern Pacific water. But the SCS water has changed a lot in its hydrographic property because of the mixing processes, heat exchange and precipitation during its long residence time in the SCS (Feng et al., 1999; Li et al., 2018). The distributions of phytoplankton and primary productivity of the SCS show great temporal and spatial variation (Ning et al., 2004). Low chlorophyll a (Chl a) and primary production are the significant characteristics of the SCS basin which is considered an oligotrophic region, and macronutrients (i.e. nitrogen) are the main limitations of phytoplankton growth and productivity (Ning et al., 2004; Lee Chen, 2005; Han et al., 2013). The excessive runoff form Pearl River can result in high N/P (nitrogen/phosphorus) ratio of > 100, shifting the nutritive state from nitrogen deficiency to phosphorus deficiency in the coastal region of SCS (Lee Chen and Chen, 2006). Dissolved iron is also a potential limitation on primary production, especially in the high nutrient low chlorophyll (HNLC) regions (Cassar et al., 2011). But on the northern slope of SCS, the concentration of dissolved iron is high enough to support the growth of phytoplankton in the surface water (Zhang et al., 2019). The northern slope of SCS is an important transition region between coastal area and SCS basin. In the summer, the shelf water intrusion is an important process changing the nutritive state in the northern slope region of SCS (He et al., 2016; Lee Chen and Chen, 2006). But so far, the NCP enhancement caused by this process is still unknown.

Previous studies about the organic carbon export in the SCS were mostly conducted on particulate organic carbon (POC) flux (e.g., Bi et al., 2013; Cai et al., 2015; Chen et al., 1998; Chen et al., 2008; Ma et al., 2008; Ma et al., 2011). Little research has been conducted on NCP in the SCS to date. Chou et al. (2006) estimated NCP in the northern SCS during the summertime to be 4.47 mmol C m^{-2} d^{-1} based on the time change rate of dissolved inorganic carbon (DIC) in the mixed layer at the South East Asia Time-Series Station (SEATS) from 2002 to 2004. Wang et al. (2014) used GPP and community respiration data from a light/dark bottle incubation experiment to calculate NCP in the northern SCS and obtained a range from −179.0 to 377.6 mmol O_2 m^{-2} d^{-1} (− 129.7 to 273.6 mmol C m^{-2} d^{-1}). Huang et al. (2018) estimated monthly NCP from July 2014 to July 2015 based on in situ O_2 measurements on an Argo profiling float and reported the cumulative NCP to be 0.29 mol C m^{-2} $month^{-1}$ (9.67 mmol C m^{-2} d^{-1}) during the northeast monsoon period and 0.17 mol C m^{-2} $month^{-1}$ (5.67 mmol C m^{-2} d^{-1}) during the southwest monsoon period in the SCS basin. However, most of these studies in the SCS were constrained by methodological factors attributed to discrete sampling and cannot reveal the rapid productivity response to highly dynamic environmental fluctuations of coastal systems. Discrete sampling suffers from low spatial resolution, and cannot adequately resolve variabilities caused by small-scale physical or biological processes in dynamic marine systems. In addition, each of the three methods for NCP estimate mentioned above has its limitation. DIC-based NCP estimate is not suitable for the coastal region, because instead of biological metabolism, the terrestrial runoff can be the strongest factor influencing the DIC in the coastal system (Mathis et al., 2011). The inavoidable difference between in situ circumstance and on deck incubation condition can introduce uncertainties to the NCP derived from light/dark bottle incubation (Grande et al., 1989). Though Argo profiling float partly gets rid of the limitation of discrete sampling, it's hard to control its movement in the study region. However, no high-resolution measurement of NCP has been reported for the SCS so far.

In this paper, we present high-resolution NCP estimates in the northern slope region of the South China Sea based on continuous shipboard dissolved O_2/Ar measurements. We discuss the regulating factors of NCP based on ancillary measurements of other hydrographic parameters. Our high-resolution measurements caught the rapid response of the ecosystem to the episodic nutrient supply induced by eddies and help us to quantify the contribution of eddy-entrained shelf water intrusion to NCP in the summer cruise.

2. Methods

2.1 Continuous underway sampling and measurement

Continuous measurements of dissolved O_2, Ar, and CO_2 were obtained using membrane inlet mass spectrometry (MIMS, HPR 40, Hiden Analytical, UK) (Tortell, 2005) onboard the *RV* 'Nanfeng' during two cruises in the northern slope region of the South China Sea (Figures 1a, 1b) from 13 to 23 October 2014 and from 13 to 29 June 2015. In addition, a cyclonic-anticyclonic eddy pair was observed in June 2015 (Figure 1c) and resulted in dramatic influences on the study region.

We developed a continuous shipboard measurement system of dissolved gases following the method described by Guéguen and Tortell (2008). Surface seawater was collected continuously using the ship's underway intake system (~5 m depth) and was divided into different lines for various underway scientific measurements. Seawater from the first line passed through a chamber at a flowrate of 2–3 L min^{-1} to remove macroscopic bubbles and to avoid pressure bursts. A flow of ~220 mL min^{-1} was continuously pumped from the chamber using a Masterflex Peristaltic Pump equipped with L/S® multichannel cartridge pump heads (Cole Parmer). In order to minimize the O_2/Ar fluctuations due to temperature effects and water vapor pressure variations, the water samples flowed through a stainless steel coil (~6 m) with 0.6 mm wall thickness immersed in a water bath (Shanghai Bilon Instrument Co. Ltd, China) to achieve a constant temperature (~2 ºC below the sea surface temperature), which avoided temperature-induced supersaturation and subsequent bubble formation. Then the water samples were introduced into a cuvette with a silicone membrane mounted on the inside. The analyte gases were monitored by a Faraday cup detector in the vacuum chamber after diffusion through the silicone membrane, and the signal intensities at the relevant mass to charge (m/z) ratios (32, 40 and 44 for O_2, Ar and

CO_2, respectively) were recorded by MASsoft. Based on the continuous measurement of 50 L air-equilibrated seawater, the long-term signal stability (measured as the coefficient of variation) over 12 h was 1.57 %, 3.75 % and 2.21 % for O_2, Ar and CO_2, respectively. Seawater from the second line passed through a flow chamber, where an RBR Maestro (RBR, Canada) was installed to continuously record temperature, salinity, dissolved oxygen (DO), and Chl a. We didn't obtain continuous DO data in October 2014 because the DO sensor of RBR broke down during this cruise. A third line was used to drain the excess seawater. Underway pipelines were flushed with freshwater or bleach every day, to avoid possible in-lines biofouling. The data from the underway transects were exported to spreadsheets and compiled into 5 min averages, and the comparisons of the gas data with other hydrographic variables were based on the UTC time recorded for each measurement.

The O_2/Ar ratio measurements were calibrated with air-equilibrated seawater samples at about 6–8 h intervals to monitor instrument drift and calculate $\Delta(O_2/Ar)$. These air-equilibrated seawater samples were prefiltered (0.22 μm) and bubbled with ambient air for at least 24 h to reach equilibrium at sea surface temperature (Guéguen and Tortell, 2008). For calibration, 800 mL of air-equilibrated seawater sample was transferred into glass bottles and immediately drawn into the cuvette, where the first 200 mL of the sample was used to flush the cuvette and pipelines. After 3 min recirculation of the sample, the average signal intensity was obtained to calculate O_2/Ar. During the course of measurements, flow rate and the temperature of water bath were both kept the same as the underway measurements. The precision of MIMS-measured O_2/Ar was 0.22 %, based on analyses of 20 duplicate samples in the laboratory test, which is comparable to previous studies and sufficient to detect biologically driven gas fluctuations in seawater (Tortell, 2005).

The instrumental CO_2 ion current was calibrated at about 12–24 h intervals using equilibrated seawater standards as per Guéguen and Tortell (2008) during the survey in June 2015. Prefiltered seawater (0.22 μm) was gently bubbled with dry CO_2 standards (200, 400, and 800 ppm, provided by the Chinese National Institute of Metrology) at in situ temperature. After 2 days of equilibrium, these standards were analyzed by MIMS following the same procedure for measuring air-equilibrated seawater samples to obtain a calibration curve between CO_2 signal intensity and mole fraction. The reproducibility of these measurements was better than 5 % within 15 days. Then we used the empirical equations reported by Takahashi et al. (2009) to convert the CO_2 mole fraction derived from the calibration curve to the in situ partial pressure of CO_2 ($p$$CO_2$).

Chlorophyll-a (Chl a) data from the RBR sensor were linear calibrated against extracted Chl a measurements of discrete seawater samples taken from the same seawater outlet as for MIMS measurements. Samples were filtered through polycarbonate filters (0.22 μm). The filter membranes were then packed with pre-sterilized aluminum foil and stored in a freezer (−20 °C) until extraction by acetone and analysis using a fluorimetric method (F-4500, HITACHI, Japan) described by Parsons (1984). The mean residual of this calibration was 0.00 ± 0.07 μg L^{-1}.

2.2 Estimation of NCP based on O_2/Ar measurements

NCP in the mixed layer was estimated by the O_2/Ar mass balance from continuous measurements. Due to similar physical properties of O_2 and Ar, $\Delta(O_2/Ar)$ is used as a proxy of the biological O_2 supersaturation and is defined as (Craig and Hayward, 1987):

$$\Delta(O_2/Ar) = \frac{([O_2]/[Ar])}{([O_2]/[Ar])_{eq}} - 1$$

where $[O_2]/[Ar]$ is the measured dissolved O_2/Ar ratio of the mixed layer and $([O_2]/[Ar])_{eq}$ is the measured dissolved O_2/Ar ratio of the air-equilibrated seawater samples. $\Delta(O_2/Ar)$ is the percent deviation of the measured O_2/Ar ratio from the equilibrium. Assuming a steady state and negligible physical supply, NCP is the air–sea biological O_2 flux and can be estimated as (Reuer et al., 2007):

$$NCP\ (mmol\ C\ m^{-2}\ d^{-1}) \approx k_{O_2} \cdot [O_2]_{sat} \cdot \Delta(O_2/Ar) \cdot r_{C:O_2} \cdot \rho$$

where k_{O_2} is the weighted gas transfer velocity of O_2 (m d^{-1}); $[O_2]_{sat}$ denotes the saturation concentration of dissolved O_2 (μmol kg^{-1}) in the mixed layer, which is calculated based on temperature and salinity (Weiss, 1970); $r_{C:O_2}$ is the photosynthetic quotient of C and O_2 and was reported as 1:1.38 in the SCS (Jiang et al., 2011); ρ is seawater density in units of kg m^{-3} (Millero and Poisson, 1981). We estimated k_{O_2} using the European Centre for Medium-Range Weather Forecasts (ECWMF) wind-speed reanalysis data product with a 0.25° × 0.25° grid (https://www.ecmwf.int), the parameterization by Wanninkhof (1992), and the gas exchange weighting algorithm by Teeter et al. (2018). Teeter et al., (2018) pointed out that modern O_2/Ar method does not strongly rely on the steady state assumption. When this assumption is violated, our estimate does not represent the actual daily NCP but rather an estimate of NCP weighted over the residence time of O_2 in the mixed layer and along the path of the water parcel during that period. Thus the residence time of O_2 in the mixed layer is an important implication of the weighted timescale of NCP before the measurement of O_2/Ar. The residence time of O_2 (τ, d) in the mixed layer is estimated as the ratio of mixed layer depth (MLD, m) to gas transfer velocity of O_2 (k_{O_2}, m d^{-1}) (Jonsson et al., 2013).

2.3 Ancillary measurements and calculations

Surface water samples for the nutrient analysis were collected from Niskin bottles mounted on the CTD, where the samples were filtered through acid-cleaned acetate cellulose filters (pore size: 0.4 μm). The filtrates were poisoned by $HgCl_2$ and stored in the dark at 4 °C. In the laboratory, the nutrients were determined photometrically by an auto-analyzer (QuAAtro, SEAL Analytical, Germany) with a precision better than 3 %. The MLDs were defined by the $\Delta\sigma_t$ = 0.125 kg m^{-3} criterion (Monterey and Levitus, 1997). The subsurface chlorophyll maximum layer (SCML) was observed using the fluorescence sensor mounted on the CTD, and it usually occurs at the bottom of euphotic layer (Hanson et al., 2007; Liao et al., 2018; Teira et al., 2005). Because no PAR (Photosynthetically Available Radiation) data were obtained in two cruises, we decided to regard the depth of SCML as the euphotic depth (Z_{eu}). The MLDs and the SCML were calculated at the stations where the vertical CTD casts were made. The MLDs for underway data between CTD stations was calculated using

删除的内容: excellent

删除的内容: past month

域代码已更改

linear interpolation based on the distance between the underway points and nearest CTD stations. We matched the underway data to each CTD location using a combination of latitude/longitude threshold (latitude/longitude of CTD station ± 0.05°) and time threshold (end/start of stationary time ± 1 h), then took the averages of these underway data for further analysis with discrete nutrient concentrations.

The daily satellite chlorophyll data were obtained from the Copernicus website (https://resources.marine.copernicus.eu). The product we used was provided by ACRI–ST company (Sophia Antipolis, France), with a space-time interpolation (the "Cloud Free"). Daily and 8-day PAR data collected by MODIS-Aqua sensor were obtained from NASA's ocean color website (https://oceancolor.gsfc.nasa.gov/l3). The spatial resolution of both satellite products is 4 km, and we match the satellite PAR with CTD station by choosing the closet PAR data point to the CTD location. A light attenuation coefficient (K_d, m^{-1}) was used to estimate the average PAR in the mixed layer (Kirk 1994; Jerlov 1976):

$$K_d = \frac{4.605}{Z_{eu}}$$

域代码已更改

3. Results and Discussion

3.1 Distributions of hydrographic parameters and gases

The distributions of temperature, salinity, Chl a, and $\Delta(O_2/Ar)$ during the autumn cruise (October 2014) are shown in Figure 2. Sea surface temperature (SST) ranged from 26.96 °C to 28.53 °C with an average of 27.82 ± 0.33 °C. Sea surface salinity (SSS) ranged from 33.28 to 34.11 with the low values occurring in the southeast of the region. Chl a concentration ranged from 0.01 to 0.71 μg L^{-1} and was in an average of 0.18 ± 0.13 μg L^{-1}, which was comparable to the 11-year mean value (~ 0.2 mg m^{-3}) in the same region in October reported by Liu et al. (2014). $\Delta(O_2/Ar)$ values were in the range of −2.9–4.9 % (avg. 1.1 % ± 0.9 %) and most areas were slightly oversaturated (Figure 2d). In addition, please note that all averages we have published in this paper are reported in the format of *mean ± standard deviation*.

带格式的：上标

In June 2015, SST ranged from 29.28 °C to 32.24 °C and was in an average of 30.88

± 0.59 °C (Figure 3a). SSS ranged from 30.81 to 34.16. Transect 3 was significantly characterized by low salinity (Figure 3b). He et al (2016) reported that this phenomenon was influenced by the eddy-entrained Pearl River plume (shelf water) injected into the SCS. Chl a varied in a range of 0.09–0.58 μg L^{-1} in the study region. Under the influence of this plume water, Chl a values higher than 0.30 μg L^{-1} were observed along Transect 3 (Figure 3c). In contrast, Chl a was in the range of 0.09–0.18 μg L^{-1} along Transect 1 and 2. It was obvious that DO was much higher in the east side than the west side in the study region (Figure 3d). $\Delta(O_2/Ar)$ ranged from −3.9–13.6 %. Most of the $\Delta(O_2/Ar)$ values were positive in the study region (avg. 2.7 % ± 2.8 %), whereas the negative values were concentrated along Transect 4 (Figure 3f). $\Delta(O_2/Ar)$ along Transect 3 was in an average of 7.2 % ± 2.6 %, significantly higher than that of other transects (Figure 3f). pCO_2 exhibited a high degree of spatial and temporal variability and the high values mostly occurred on the west side of the study region (Figure 3e). Resulting from the considerable low pCO_2 in Transect 3, the average pCO_2 (323 ± 93 μatm) in the study region was lower than those reported previously, i.e., 350–370 μatm by Zhai et al (2009) and 340–350 μatm by Rehder and Sues (2001). Due to the influence of the plume water, the average pCO_2 in Transect 3 was 222 ± 33 μatm, with a range of 144–321 μatm. In the summer, shelf water mixed with Pearl River plume is the most important factor influencing pCO_2 in the coastal and shelf region of northern SCS, which can result in the pCO_2 values as low as 150 μatm (Li et al., 2020). Here we apply an average atmospheric pCO_2 of 382 μatm that observed in July 2015 in the northern SCS (Li et al., 2020) to calculate the pCO_2 difference (ΔpCO_2) between the surface water and the atmosphere. ΔpCO_2 ranged from −238 to −61 μatm along Transect 3, indicative of a strong CO$_2$ sink.

删除的内容: biological

3.2 Mixed layer depth, euphotic depth and residence time of O_2 in the mixed layer

The mixed layer depth (MLD), euphotic depth (Z_{eu}) and residence time of O_2 (τ) in the mixed layer at CTD stations of two cruises are shown in Table 1 and 2 respectively. In autumn 2014, MLD ranged from 27 to 81 m, with an average of 55 ±

15 m (Table 1). The average Z_{eu} was 74 ± 12 m, approximately 20 m deeper than MLD (Table 1). The residence time of O_2 in the mixed layer ranged from 3 to 13 d (Table 1), comparable to a reasonable range of 1–2 weeks reported by previous studies (Izett et al., 2018; Manning et al., 2017). The average residence time of O_2 was 9 ± 3 d, indicating that our estimate generally quantified NCP over 9 days prior to the underway observation of O_2/Ar in the mixed layer during this cruise.

The average MLD in June 2015 was just 18 ± 6 m, shallower than that of October 2014 (Table 2). Significant shallow MLD occurred at two stations (J-10, J-11) located in Transect 3 (Table 2, Figure S1f). The low-salinity shelf water intrusion is the main cause of this shallow MLD of 8 m. The average Z_{eu} was 58 ± 18 m, approximately 40 m deeper than the MLD (Table 2). The residence time of O_2 in the mixed layer ranged from 2 to 12 d (Table 2), indicating a fast gas exchange in some stations. In addition, we also observed relatively obvious subsurface O_2 maxima in Transect 1 and 2 in summer 2015. But this phenomenon didn't exist in autumn 2014.

In both cruises, the Z_{eu} was observed obviously deeper than MLD. This result partly suggests that light availability may not be a limitation of NCP in the northern slope of SCS. Especially in the summer, Z_{eu} extended to 2–7 times of MLD (Table 2), ensuring sufficient illumination in the mixed layer. But in the autumn when the thickness of mixed layer account for about 74 % of euphotic layer, the average light intensity in the mixed layer might be influenced by the exponentially light attenuation along depth.

带格式的: 左侧: 3.17 厘米, 右侧: 3.17 厘米

3.3 NCP in autumn and summer

In October 2014, NCP in the northern slope of the SCS ranged from −29.2 to 42.7 mmol C m^{-2} d^{-1} (avg. 11.5 ± 8.7 mmol C m^{-2} d^{-1}) and most of the region was net autotrophic (Figure 4a). The estimated NCP based on the O_2/Ar values measured in this cruise is about 34 % of the net primary production rates of 34.3 mmol C m^{-2} d^{-1} measured by ^{14}C bottle incubation (Sun X., personal communication), which was in agreement with previous research (Quay et al., 2010).

The average NCP in the study region was 11.6 ± 12.7 mmol C m^{-2} d^{-1} with a range of −27.6–61.4 mmol C m^{-2} d^{-1} in June 2015. A high NCP level was observed along Transect 3 (Figure 4b). Eddy-entrained shelf water brought a large amount of terrigenous nutrients from the shelf to the slope region along Transect 3 (He et al., 2016). The average nitrate (NO_3^-) and nitrite (NO_2^-) concentrations in the surface water of Transect 3 were 2.31 ± 0.70 μmol L^{-1} and 0.04 ± 0.01 μmol L^{-1} respectively (Figure S1a, S1b); both values were much higher than those found in the other three transects where NO_3^- was in a range of < 0.03–0.69 μmol L^{-1} and NO_2^- was mostly below the detection limit. Li et al. (2018) reported that the entire Transect 3 and part of Transect 4 were dominated by shelf water at the surface and we estimated NCP over these regions where salinity lower than 33.0 as 23.8 ± 10.7 mmol C m^{-2} d^{-1} on average. We also observed a warm eddy (anti-cyclone) covering most stations in Transects 1 and 2 (Figure 1b, 1c) during our survey in June 2015 (Chen et al., 2016). Anti-cyclonic eddies can cause downwelling, deepening of the thermocline, and blocking of the supply of nutrients from the deeper water (Ning et al., 2008; Shi et al., 2014). Consequently, a warm eddy is expected to result in an oligotrophic condition in the surface water associated with low Chl a concentrations and low production (Ning et al., 2004). As a result, in the summer of 2015, the observed NO_2^-, NO_3^-, and PO_4^{3-} (phosphate) concentrations were almost below the detection limit in Transects 1 and 2 (Figure S1a, S1b, S1d). NCP in Transect 1 and 2 was at a very low level (avg. 2.8 ± 2.7 mmol C m^{-2} d^{-1}). Because of the significant high values of NCP over the regions with shelf water intrusion, our NCP result in the summer of 2015 is averagely higher than the previous values of 4.47 mmol C m^{-2} d^{-1} and 0.17 mol C m^{-2} $month^{-1}$ (5.67 mmol C m^{-2} d^{-1}) based on DIC budget and Argo-O_2 respectively in the SCS (Chou et al., 2006; Huang et al., 2018). However, NCP estimates based on both methods mentioned above suffer from poor temporal and spatial coverage and do not allow for revealing rapid changes in shelf systems. In contrast, continuous measurements of O_2/Ar allow us to capture rapid variations in NCP along Transect 3 and resolve short-term productivity responses to environmental fluctuations.

3.4 Distribution of various parameters along representative transects

We chose Transect 5 (Figure 1a) observed in October 2014 and Transect 4 (Figure 1b) observed in June 2015 to show the distribution of various parameters.

The distribution of Chl a, $\Delta(O_2/Ar)$, and NCP showed similar trend along Transect 5 in October 2014 (Figure 5). There's a trough of temperature, showing a maximum drawdown of ~ 0.6 °C compared to the average temperature in the study region (Figure 5a). But the temperature fluctuations shown here are too small to reflect a significant upwelling that can easily cause ~ 2 °C drawdown of temperature in the upper layer (Lin et al., 2013; Manning et al., 2017; Ning et al., 2004). A spike of Chl a occurred between 115.6°E and 115.7°E and was coincident with the peaks of $\Delta(O_2/Ar)$ and NCP (Figure 5b, 5c). The highest surface concentration of ammonium (NH_4^+) of 0.35 μmol L^{-1} was also observed between 115.6°E and 115.7°E in this transect and was predominantly higher than the concentrations (0.07–0.17 μmol L^{-1}) in the other regions of this cruise (Figure 5c, S2b). Because no significant obduction processes (i.e., upwelling, entrainment, and diapycnal mixing) were reported in this region, the most likely source of this abundant NH_4^+ was in situ regeneration. The excretion of zooplankton and the bacterial decomposition of organic matter were considered to be the main mechanisms for the release of NH_4^+ into the surface water (La Roche, 1983; Clark et al., 2008). Ammonium is an important nitrogen source of phytoplankton growth, which can be quickly utilized by phytoplankton, and contributes to primary production (Dugdale and Goering, 1967; Tamminen, 1982). Though we only got nutrient data at two CTD stations in this transect, the result partly indicated that higher ammonium could result in higher $\Delta(O_2/Ar)$ and NCP.

A similar distribution pattern of Chl a, NCP, and $\Delta(O_2/Ar)$ was observed along Transect 4 in June 2015, whereas $p\mathrm{CO_2}$ showed the opposite trend for these three parameters (Figure 6b, 6c). Low salinity (lower than 33) existed at both southern and northern end of this transect (Figure 6a). The concentration of dissolved inorganic nitrogen (DIN, $NO_3^- + NO_2^- + NH_4^+$) in the surface water was 0.81 μmol L^{-1} and 0.27 μmol L^{-1} at the southern and northern end respectively, which was higher than the concentrations in other stations of this transect (Figure 6c). These results indicate that shelf water is imported at the northern and southern end of this transect, along with higher levels of Chl a and NCP (Figure 6c). A sharp drop in the temperature and an increase in salinity occurred from 19.7°N to 19.8°N and from 21°N to 20.7°N (Figure 6a), manifesting an upwelling over this area together with dramatic spikes in pCO_2 and associated decrease in $\Delta(O_2/Ar)$ (Nemcek et al., 2008) (Figure 6b). A localized cold eddy was considered to be the cause of this upwelling (Figure 1c), and most regions of Transect 4 were dominated by upwelling and showed negative sea level height anomaly (Chen et al., 2016; He et al., 2016), resulting in a maximum temperature drawdown of ~1.6 °C in the mixed layer.

Vertical mixing is considered the largest source of error in O_2/Ar-based NCP estimates because the upwelled subsurface water with different O_2/Ar signatures can produce either an overestimation or an underestimation of NCP in the mixed layer (Cassar et al., 2014; Izett et al., 2018). Former researches usually ignored the underestimated negative NCP that caused by vertical mixing (Giesbrecht et al., 2012; Reuer et al., 2007; Stanley et al., 2010). Cassar et al. (2014) presented a N_2O-based correction method of O_2/Ar and NCP for vertical mixing. Although this method has been successfully adopted by Izett et al. (2018) in the Subarctic Northeast Pacific, it is not suitable for our study region. This is because it is basically applicable in areas where the depths of euphotic zone and mixed layer are similar, and this method is not suitable for oligotrophic regions (Cassar et al., 2014). The SCS is recognized as an oligotrophic region and the depth of the euphotic zone can be 2–7 times that of the mixed layer in our study region in the summer. In addition, in the region (e.g. the SCS basin) where subsurface oxygen maximum exists, the applicability of N_2O-based correction method is limited (Izett et al., 2018). In Transect 4, the regions with negative NCP and the regions with salinity higher than 33.5 and temperature lower than 30 °C are defined as influenced by upwelling. If we neglect these regions in Transect 4, the average NCP in June 2015 can slightly raise to 12.4 ± 12.3 mmol C m^{-2} d^{-1}. If we also remove the influence of shelf water intrusion by neglecting the regions with salinity lower than 33, the average NCP can sharply decrease to 5.0 ± 6.2 mmol C m^{-2} d^{-1}, which was similar to the results of 4.47 mmol C m^{-2} d^{-1} and 0.17 mol C m^{-2} $month^{-1}$ (5.67 mmol C m^{-2} d^{-1}) reported in previous researches in the same season (Chou et al., 2006; Huang et al., 2018). Here we regard 5.0 ± 6.2 mmol C m^{-2} d^{-1} as the background value of NCP in the study region. Since an average NCP of 23.8 ± 10.7 mmol C m^{-2} d^{-1} was observed over the regions with salinity lower than 33, we can conclude that the summer shelf water intrusion significantly promoted NCP by about 376 % in June 2015.

3.5 Factors influencing NCP in the SCS

The SCS is an oligotrophic region with low biomass and primary production (Lee Chen, 2005; Ning et al., 2004). Previous research has shown that the nutrient, especially nitrogen and phosphorus, is the most important factor controlling and limiting the phytoplankton biomass and primary production in the SCS (Ning et al., 2004; Lee Chen, 2005; Lee Chen and Chen, 2006; Han et al., 2013). After neglecting the two CTD stations (J-14, J-15) with negative NCP influenced by upwelling in June 2015, we performed a principal component analysis (PCA) to determine the dominant factors influencing NCP in both cruises. In October 2014, DIN (0.741), $\Delta(O_2/Ar)$ (0.858), and NCP (0.979) were significantly loaded on Factor 1, indicating a potential relationship among these three variables (Figure 7a, Table S1b). The correlation coefficient between DIN and NCP was 0.706 ($p < 0.01$, Table S1a), which was significantly higher than the coefficient between NCP and the other variables, except for $\Delta(O_2/Ar)$ and temperature; this indicated that DIN was an important factor influencing NCP in this cruise. Another two nutrients – dissolved silicate (DSi, SiO_3^{2-}) and dissolved inorganic phosphorus (DIP, PO_4^{3-}) – had no correlations ($p > 0.05$) with NCP (Table S1a). In June 2015, Factor 1 showed a strong loading by DIN (0.876), Chl a (0.950), DO (0.927), $\Delta(O_2/Ar)$ (0.902), and NCP (0.909), whereas salinity (−0.936) and pCO_2 (−0.908) were negatively loaded on Factor 1 (Figure 7b, Table S2b). The injection of low salinity shelf water appeared to have a strong effect on the study region because significant negative correlations were observed between salinity and DIN, Chl a, $\Delta(O_2/Ar)$, and NCP (Table S2a). DIN had strong correlations with NCP, $\Delta(O_2/Ar)$, and Chl a, with the correlation coefficients of 0.747, 0.910, and 0.754, respectively (Table S2a), indicating that DIN was the dominant factor controlling the growth of phytoplankton and primary production in this cruise. DSi (0.582) and DIP (−0.601) were both moderately loaded on Factor 2 (Figure 7b, Table S2b) and had no correlations with NCP ($p > 0.05$, Table S2a). These results suggested the key role of nitrogen in regulating $\Delta(O_2/Ar)$, NCP, and phytoplankton biomass in the SCS. The supply of nitrogen may stimulate the growth of phytoplankton in the SCS and nitrogen is an important participant in photosynthesis and a basic element that contributes to the increase in primary production (Dugdale and Goering, 1967; Lee Chen, 2005; Lee Chen and Chen, 2006; Han et al., 2013).

Coupled with biochemical variations, physical processes also play important roles in the slope region of the SCS by transporting abundant nutrient-rich shelf water into the SCS and bringing deep water to the surface by enhancing water mixing (Chen and Tang, 2012; Ning et al., 2004; Pan et al., 2012). The surface waters in the slope region of the northern SCS are primarily composed of waters originating from SCS water, Kuroshio water, and shelf water (Li et al., 2018). In the summer, the shelf water exists where the potential density anomaly is lower than 20.5 kg m^{-3} (Li et al., 2018). In the autumn, there is a weak offshore transport of the shelf water in the SCS and the salinity of the water mixed with the shelf water is usually lower than 33 (Fan et al., 1988; Uu and Brankart, 1997; Su and Yuan, 2005). In October 2014, the observed surface salinity was in a range of 33.28 to 34.11; thus the surface waters were mainly derived from mixing of the Kuroshio water and the SCS water. In the summer of 2015, a cyclonic-anticyclonic eddy pair was observed in the study region (Figure 1c). Low-salinity shelf water mixed with the intruding plume water from the Pearl River in the upper 50 m and was transported to the slope and basin along the intersection of the two eddies (Chen et al., 2016; He et al., 2016; Li et al., 2018). In both seasons, the surface waters in the study region were generally found to be nitrogen deficient, with NO_2^- at < 0.01–0.04 μmol L^{-1} (Figure S2a, S1b), NO_3^- at < 0.03–2.82 μmol L^{-1} (Figure S1a), and NH_4^+ at 0.04–0.35 μmol L^{-1} (Figure S2b, S1c). The concentrations of NO_2^- and NO_3^- were below the detection limit at almost 80% of the sampling stations during both cruises. Due to the injection of shelf water with low salinity and abundant terrestrial nutrients, significant high concentrations of NO_3^- and NO_2^- were observed along Transect 3 in June 2015 (Figure S1a, S1b) where the shelf water was intruded by eddies (Chen et al., 2016; He et al., 2016). Such transport processes from the inner shelf to the slope region have a profound influence on nutrient dynamics and biological productions (He et al., 2016). The water that was influenced by shelf water with a potential density anomaly lower than 20.25 kg m^{-3} and salinity lower than 33.0 had high concentrations of DIN (Figure 8a). At the 6 stations (in the red circle of Figure 8a) that were intruded by shelf water and characterized with surface salinity lower than 33.0, we obtained an average surface DIN concentration of 1.82 ± 1.16 (0.27–3.01) μmol L^{-1}, which was significantly higher than the mean of 0.10 ± 0.03 (0.04–0.16) μmol L^{-1} at other stations (independent samples t-test, $p < 0.01$). After neglecting the two stations (J-14, J-15) influenced by upwelling, a strong correlation between NCP and DIN was observed during the cruise of June 2015 (r = 0.747, $p < 0.01$), with higher NCP (avg. 15.4 ± 4.5 mmol C m^{-2} d^{-1}) occurred at the stations where shelf water intruded, consistent with the DIN concentration higher than 0.27 μmol L^{-1} (Figure 8b). At other stations without the influence of shelf water, the average NCP was just 2.3 ± 1.7 mmol C m^{-2} d^{-1}. These results furtherly suggest that the supply of DIN from shelf water can greatly stimulate the primary production at these stations, resulting in the NCP increase of nearly 7 times compared to other stations.

The correlations between NCP and sea surface temperature and salinity also support the influence of physical forcing on NCP. In June 2015, we obtained strong negative correlations between NCP and salinity (Figure 9d). NCP significantly increased in the water with salinity lower than 33 (Figure 9d). Temperature had weak correlations with NCP (Figure 9c), and the negative NCP values were concentrated in the water with temperatures below 30.5 °C and salinity values over 33.5 (Figure 9c, 9d). This surface water was mostly observed along Transect 4 where vertical mixing caused by a cold eddy brought deep water to the surface. The undersaturated $\Delta(O_2/Ar)$ entrained by deep water caused the negative NCP estimates at the surface, resulting in a considerable underestimation of NCP. Unlike in June 2015, all the correlations were very weak between NCP and temperature, salinity in October 2014 (Figure 9a, 9b).

The Kuroshio water and the SCS water had similar hydrological characteristics and their mixing in October 2014 may not have resulted in significant changes in the hydrological characteristics of the surface water.

The nutrient concentrations and hydrographic characteristics we observed just reflect the marine environment at the moment of sampling, partly contradicting our estimates that quantified NCP over a period prior to the observation. Especially for the regions with significant influence of shelf water in June 2015, tracking the history of shelf water intrusion is important. We used daily satellite Chl a to monitor the movement of shelf water and roughly set Chl a $\geq \sim 0.2$ μg L^{-1} as the criterion of shelf water (Figure S3). On 10 June 2015, the shelf water began to influence the northern end (J-9) of Transect 3 and most part of Transect 4, then it extended to the southern end of Transect 3 and Transect 4 where J-12 and J-13 located on 13 June (Figure 1b, S3). Till 25 June when we finished the observation of Transect 4, the entire Transect 3 (J-9 to 12) as well as J-13 and J-16 had kept been dominated by shelf water for more than 10 days (Figure 1b, S3). We concluded these findings in Table 3, along with the mixed layer O_2 residence time (τ) and the difference (Δday) between the date of observation and the start date of shelf water intrusion at stations with surface salinity lower than 33. Δday can represent the duration of the shelf water intrusion at each station before our observation. The mixed layer O_2 residence time at most stations listed in Table 3 is shorter than or equivalent to Δday. This result suggests that our estimate has appropriately integrated the NCP during the period of shelf water intrusion, which can effectively reflect the influence of shelf water on productive state on the northern slope of SCS in the summer.

Light may also play a role in the primary production. The MLD is considered a driver of light availability in the mixed layer (Cassar et al., 2011; Hahm et al., 2014). The euphotic layer was averagely 40 m thicker than the mixed layer in the study region during the summer cruise, thus it’s not very significant to discuss the light limitation in June 2015. We conducted an analysis of light availability based on daily satellite-PAR data and NCP in October 2014. To minimize the influence of DIN concentrations, we selected 9 stations where surface DIN concentration in the range of

0.10–0.17 μmol L^{-1}. The average surface PAR (mol m^{-2} d^{-1}) at each station was integrated over the residence time of O_2 before our observation. Then an average PAR in the mixed layer was calculated based on K_d. At the selected stations, the surface PAR varies over a range of 38.6–42.2 mol m^{-2} d^{-1}, while the average PAR in the mixed layer (ML PAR) ranged from 8.7 to 13.3 mol m^{-2} d^{-1} (Table 4). There's no significant correlation between the average PAR and NCP in the mixed layer (Table 4), partly suggesting that light intensity may not be a factor on NCP in the autumn. Light availability in the northern slope region of SCS is enough to support the primary production of phytoplankton.

4 Conclusion

The distribution of $\Delta(O_2/Ar)$ and NCP on the northern slope of the SCS was strongly affected by nutrient availability, especially nitrogen. The nitrogen limitation on NCP was found both in the autumn and summer. In June 2015, we observed strong biological responses to the supply of nitrogen induced by eddy-entrained shelf water intrusion. NCP in the region with the influence of shelf water was 23.8 ± 10.7 mmol C m^{-2} d^{-1} on average, with a maximum of 61.4 mmol C m^{-2} d^{-1}. In addition, dynamic processes such as vertical mixing caused the errors of NCP estimates. Removing the regions with the influence of shelf water intrusion and vertical mixing, the average NCP in other regions was 5.0 ± 6.2 mmol C m^{-2} d^{-1}. This value agrees well with previously published NCP estimates for the study area. Our results also reveal the rapid response of ecosystem to physical processes. The summer shelf water intrusion may significantly promote NCP by 376 % in the study region. This is the first report that quantifies the contribution of shelf water intrusion to NCP on the northern slope of the SCS in the summer. Because of the sufficient illumination in the tropical SCS, light availability may not be a significant limitation on NCP in both seasons. The high-resolution NCP estimates derived from continuous measurements of O_2/Ar presented in this paper are of significance for understanding the carbon cycling in the highly dynamic system of the SCS.

Data Availability

All data presented in this manuscript are available on Weiyun.com (link: https://share.weiyun.com/ZtbQMNGl, password: p7rj36)

Author contribution

Guiling Zhang and Yu Han designed and set up the underway measurement system. Wenjing Zheng attended both cruises (in June 2015 and October 2014) in the South China Sea, and was mainly responsible for operating the underway measurement system during the cruises. Sumei Liu provided the nutrients data of both cruises. Chuan Qin attended the cruise in June 2015 and prepared the manuscript with contributions from all co-authors.

Acknowledgments

The authors wish to thank the crew of the *R/V* “Nanfeng” for the assistance with the collection of field samples and Professor Xiaoxia Sun for providing the ^{14}C-PP data. Professor Michael Bender and Bror Jonsson are acknowledged for constructive suggestions on the continuous O_2/Ar measurement system and the calculation of O_2/Ar-based NCP. This study was funded by the National Science Foundation of China through Grant Nos. 41776122, by the Ministry of Science and Technology of China through Grant Nos. 2014CB441502, by the Fundamental Research Funds for the Central Universities (No. 201562010), and by the Taishan Scholars Programme of Shandong Province (No. 201511014) and the Aoshan Talents Programme of the Qingdao National Laboratory for Marine Science and Technology (No. 2015ASTP-OS08).

Competing interests

The authors declare that they have no conflict of interest.

References:

Bi, Q., Du, J., Wu, Y., Zhou, J. and Zhang, J.: Particulate organic carbon export flux by $^{234}Th/^{238}U$ disequilibrium in the continental slope of the East China Sea, Acta Oceanol. Sin., 32(10), 67–73, doi:10.1007/s13131-013-0303-7, 2013.

Cai, P., Zhao, D., Wang, L., Huang, B. and Dai, M.: Role of particle stock and phytoplankton community structure in regulating particulate organic carbon export in a large marginal sea, J. Geophys. Res. Oceans, 120(3), 2063–2095, doi:10.1002/2014JC010432, 2015.

Cai, W.: Estuarine and Coastal Ocean Carbon Paradox: CO_2 Sinks or Sites of Terrestrial Carbon Incineration?, Ann. Rev. Mar. Sci., 3(1), 123–145, doi:10.1146/annurev-marine-120709-142723, 2011.

Cassar, N., Difiore, P. J., Barnett, B. A., Bender, M. L., Bowie, A. R., Tilbrook, B., Petrou, K., Westwood, K. J., Wright, S. W. and Lefevre, D.: The influence of iron and light on net community production in the Subantarctic and Polar Frontal Zones, Biogeosciences, 8(2), 227–237, doi:10.5194/bg-8-227-2011, 2011.

Cassar, N., Nevison, C. D. and Manizza, M.: Correcting oceanic O_2/Ar-net community production estimates for vertical mixing using N_2O observations, Geophys. Res. Lett., 41(24), 8961–8970, doi:10.1002/2014GL062040, 2014.

Chen, J., Zheng, L., Wiesner, M. G., Chen, R., Zheng, Y. and Wong, H.: Estimations of primary production and export production in the South China Sea based on sediment trap experiments, Chinese Sci. Bull., 43(7), 583–586, doi:10.1007/BF02883645, 1998.

Chen, W., Cai, P., Dai, M. and Wei, J.: $^{234}Th/^{238}U$ disequilibrium and particulate organic carbon export in the northern South China Sea, J. Oceanogr., 64(3), 417–428, doi:10.1007/s10872-008-0035-z, 2008.

Chen, Y. and Tang, D.: Eddy-feature phytoplankton bloom induced by a tropical cyclone in the South China Sea, Int. J. Remote Sens., 33(23), 7444–7457, doi:10.1080/01431161.2012.685976, 2012.

Chen, Z., Yang, C., Xu, D. and Xu, M.: Observed hydrographical features and circulation with influences of cyclonic-anticyclonic eddy-pair in the northern slope of the South China Sea during June 2015 (in Chinese), J. Mar. Sci., 34(4), 10–19, doi:10.3969/j.issn.1001-909X.2016.04.002, 2016.

Cheng, G., Sun, J., Zu, T., Chen, J. and Wang, D.: Analysis of water masses in the northern South China Sea in summer 2011 (in Chinese), J. Trop. Oceanogr., 33(3), 10–16, doi:10.3969/j.issn.1009-5470.2014.03.002, 2014.

Chou, W., Lee Chen, Y., Sheu, D., Shih, Y., Han, C., Cho, C., Tseng, C. and Yang, Y.: Estimated net community production during the summertime at the SEATS time-series study site, northern South China Sea: Implications for nitrogen fixation, Geophys. Res. Lett., 33(22), doi:10.1029/2005GL025365, 2006.

Clark, D. R., Rees, A. P. and Joint, I.: Ammonium regeneration and nitrification rates in the oligotrophic Atlantic Ocean: Implications for new production estimates, Limnol. Oceanogr., 53(1), 52–62, doi:10.4319/lo.2008.53.1.0052, 2008.

Craig, H. and Hayward, T.: Oxygen Supersaturation in the Ocean: Biological Versus Physical Contributions, Science, 235(4785), 199–202, doi:10.1126/science.235.4785.199, 1987.

Dugdale, R. C. and Goering, J. J.: Uptake of New and Regenerated Forms of Nitrogen in Primary Productivity, Limnol. Oceanogr., 12(2), 196–206, doi:10.4319/lo.1967.12.2.0196, 1967.

Eveleth, R., Cassar, N., Sherrell, R. M., Ducklow, H., Meredith, M. P., Venables, H. J., Lin, Y. and Li, Z.: Ice melt influence on summertime net community production along the Western Antarctic Peninsula, Deep Sea Res. Part II Top. Stud. Oceanogr., 139, 89–102, doi:10.1016/j.dsr2.2016.07.016, 2017.

Fan, L., Su, Y. and Li, F.: Analysis on water mases in the Northern South China Sea (in Chinese), Acta Oceanol. Sin., 10(2), 136–145, 1988.

Feng, S., Li, F. and Li, S.: An introduction to marine science (in Chinese), Higher Education Press, Beijing, China., 1999.

Giesbrecht, K. E., Hamme, R. C. and Emerson, S. R.: Biological productivity along Line P in the subarctic northeast Pacific: In situ versus incubation-based methods, Global Biogeochem. Cycles, 26(3), doi:10.1029/2012GB004349, 2012.

Grande, K. D., Williams, P. J. L. B., Marra, J., Purdie, D. A., Heinemann, K., Eppley, R. W. and Bender, M. L.: Primary production in the North Pacific gyre: a comparison of rates determined by the ^{14}C, O_2 concentration and ^{18}O methods, Deep Sea Res. Part A, Oceanogr. Res. Pap., 36(11), 1621–1634, doi:10.1016/0198-0149(89)90063-0, 1989.

Guéguen, C. and Tortell, P. D.: High-resolution measurement of Southern Ocean CO_2 and O_2/Ar by membrane inlet mass spectrometry, Mar. Chem., 108(3–4), 184–194, doi:10.1016/j.marchem.2007.11.007, 2008.

Hahm, D., Rhee, T. S., Kim, H. C., Park, J., Kim, Y. N., Shin, H. C. and Lee, S.: Spatial and temporal variation of net community production and its regulating factors in the Amundsen Sea, Antarctica, J. Geophys. Res. Oceans, 119(5), 2815–2826, doi:10.1002/2013JC009762, 2014.

Hamme, R. C., Cassar, N., Lance, V. P., Vaillancourt, R. D., Bender, M. L., Strutton, P. G., Moore, T. S., DeGrandpre, M. D., Sabine, C. L., Ho, D. T. and Hargreaves, B. R.: Dissolved O_2/Ar and other methods reveal rapid changes in productivity during a Lagrangian experiment in the Southern Ocean, J. Geophys. Res. Oceans, 117(C4), 92–99, doi:10.1029/2011JC007046, 2012.

Han, A., Dai, M., Gan, J., Kao, S., Zhao, X., Jan, S., Li, Q., Lin, H., Chen, C., Wang, L., Hu, J., Wang, L. and Gong, F.: Inter-shelf nutrient transport from the East China Sea as a major nutrient source supporting winter primary production on the northeast South China Sea shelf, Biogeosciences, 10(12), 8159–8170, doi:10.5194/bg-10-8159-2013, 2013.

Hanson, C. E., Pesant, S., Waite, A. M. and Pattiaratchi, C. B.: Assessing the magnitude and significance of deep chlorophyll maxima of the coastal eastern Indian Ocean, Deep. Res. Part II Top. Stud. Oceanogr., 54(8–10), 884–901, doi:10.1016/j.dsr2.2006.08.021, 2007.

He, X., Xu, D., Bai, Y., Pan, D., Chen, C. A., Chen, X. and Gong, F.: Eddy-entrained Pearl River plume into the oligotrophic basin of the South China Sea, Cont. Shelf Res., 124, 117–124, doi:10.1016/j.csr.2016.06.003, 2016.

Hu, J., Kawamura, H., Hong, H. and Qi, Y.: A Review on the currents in the South China Sea: Seasonal circulation, South China Sea warm current and Kuroshio intrusion, J. Oceanogr., 56(6), 607–624, doi:10.1023/A:1011117531252, 2000.

Huang, Y., Yang, B., Chen, B., Qiu, G., Wang, H. and Huang, B.: Net community production in the South China Sea Basin estimated from in situ O_2 measurements on an Argo profiling float, Deep Sea Res. Part I Oceanogr. Res. Pap., 131, 54–61, doi:10.1016/j.dsr.2017.11.002, 2018.

Izett, R. W., Manning, C. C., Hamme, R. C. and Tortell, P. D.: Refined Estimates of Net Community Production in the Subarctic Northeast Pacific Derived From ΔO_2/Ar Measurements With N_2O-Based Corrections for Vertical Mixing, Global Biogeochem. Cycles, 32(3), 326–350, doi:10.1002/2017GB005792, 2018.

Jiang, Z., Huang, C., Dai, M., Kao, S., Hydes, D. J., Chou, W. and Janf, S.: Short-term dynamics of oxygen and carbon in productive nearshore shallow seawater systems off Taiwan: Observations and modeling, Limnol. Oceanogr., 56(5), 1832–1849, doi:10.4319/lo.2011.56.5.1832, 2011.

Jonsson, B. F., Doney, S. C., Dunne, J. and Bender, M.: Evaluation of the Southern Ocean O_2/Ar-based NCP estimates in a model framework, J. Geophys. Res. Biogeosciences, 118(2), 385–399, doi:10.1002/jgrg.20032, 2013.

Jerlov, N. G.: Marine optics, Elsevier, Netherlands, 1976.

Kaiser, J., Reuer, M. K., Barnett, B. and Bender, M. L.: Marine productivity estimates from continuous O_2/Ar ratio measurements by membrane inlet mass spectrometry, Geophys. Res. Lett., 32(19), 1–5, doi:10.1029/2005GL023459, 2005.

Kirk, J. T.: Light and photosynthesis in aquatic ecosystems, Cambridge university press, UK, 1994.

La Roche, J.: Ammonium regeneration: its contribution to phytoplankton nitrogen requirements in a eutrophic environment, Mar. Biol., 75(2–3), 231–240, doi:10.1007/BF00406007, 1983.

Lee Chen, Y.: Spatial and seasonal variations of nitrate-based new production and primary production in the South China Sea, Deep Sea Res. Part I Oceanogr. Res. Pap., 52(2), 319–340, doi:10.1016/j.dsr.2004.11.001, 2005.

Lee Chen, Y. and Chen, H.: Seasonal dynamics of primary and new production in the northern South China Sea: The significance of river discharge and nutrient advection, Deep Sea Res. Part I Oceanogr. Res. Pap., 53(6), 971–986, doi:10.1016/j.dsr.2006.02.005, 2006.

Li, D., Zhou, M., Zhang, Z., Zhong, Y., Zhu, Y., Yang, C., Xu, M., Xu, D. and Hu, Z.: Intrusions of Kuroshio and Shelf Waters on Northern Slope of South China Sea in Summer 2015, J. Ocean Univ. China, 17(3), 477–486, doi:10.1007/s11802-018-3384-2, 2018.

Li, Q., Guo, X., Zhai, W., Xu, Y. and Dai, M.: Partial pressure of CO_2 and air-sea CO_2 fluxes in the South China Sea: Synthesis of an 18-year dataset, Prog. Oceanogr., 182, doi:10.1016/j.pocean.2020.102272, 2020.

Liao, X., Dai, M., Gong, X., Liu, X. and Huang, H.: Subsurface chlorophyll a maximum and its possible causes in the southern South China Sea, J. Trop. Oceanogr., 37(1), 45–56, doi:10.11978/2017020, 2018.

Lin, X., Guan, Y. and Liu, Y.: Three-dimensional structure and evolution process of Dongsha Cold

Eddy during autumn 2000 (in Chinese), J. Trop. Oceanogr., 32(2), 55–65, doi:10.3969/j.issn.1009-5470.2013.02.006, 2013.

Liu, M., Liu, X., Ma, A., Li, T. and Du, Z.: Spatio-temporal stability and abnormality of chlorophyll-a in the northern south china sea during 2002-2012 from MODIS images using wavelet analysis, Cont. Shelf Res., 75, 15–27, doi:10.1016/j.csr.2013.12.010, 2014.

Lockwood, D., Quay, P. D., Kavanaugh, M. T., Juranek, L. W. and Feely, R. A.: High-resolution estimates of net community production and air-sea CO_2 flux in the northeast Pacific, Global Biogeochem. Cycles, 26(4), doi:10.1029/2012GB004380, 2012.

Ma, H., Zeng, Z., He, J., Chen, L., Yin, M., Zeng, S. and Zeng, W.: Vertical flux of particulate organic carbon in the central South China Sea estimated from ^{234}Th-^{238}U disequilibria, Chinese J. Oceanol. Limnol., 26(4), 480–485, doi:10.1007/s00343-008-0480-y, 2008.

Ma, H., Zeng, Z., Yu, W., He, J., Chen, L., Cheng, J., Yin, M. and Zeng, S.: ^{234}Th/ ^{238}U disequilibrium and particulate organic carbon export in the northwestern South China Sea, Acta Oceanol. Sin., 30(3), 55–62, doi:10.1007/s13131-011-0119-2, 2011.

Manning, C. C., Stanley, R. H. R., Nicholson, D. P., Smith, J. M., Timothy Pennington, J., Fewings, M. R., Squibb, M. E. and Chavez, F. P.: Impact of recently upwelled water on productivity investigated using in situ and incubation-based methods in Monterey Bay, J. Geophys. Res. Oceans, 122(3), 1901–1926, doi:10.1002/2016JC012306, 2017.

Mathis, J. T., Cross, J. N. and Bates, N. R.: Coupling primary production and terrestrial runoff to ocean acidification and carbonate mineral suppression in the eastern Bering Sea, J. Geophys. Res. Ocean., 116(2), doi:10.1029/2010JC006453, 2011.

Millero, F. J. and Poisson, A.: International one-atmosphere equation of state of seawater, Deep Sea Res. Part A, Oceanogr. Res. Pap., 28(6), 625–629, doi:10.1016/0198-0149(81)90122-9, 1981.

Monterey, G. and Levitus, S.: Seasonal Variability of Mixed Layer Depth, NOAA Atlas NEDIS 14, U.S. Gov. Prinitng Off. D.C. [online] Available from: http://www.nodc.noaa.gov, 1997.

Nemcek, N., Ianson, D. and Tortell, P. D.: A high-resolution survey of DMS, CO_2, and O_2/Ar distributions in productive coastal waters, Global Biogeochem. Cycles, 22(2), doi:10.1029/2006GB002879, 2008.

Ning, X., Chai, F., Xue, H., Cai, Y., Liu, C. and Shi, J.: Physical-biological oceanographic coupling influencing phytoplankton and primary production in the South China Sea, J. Geophys.

Res. Oceans, 109(10), doi:10.1029/2004JC002365, 2004.

Ning, X., Peng, X., Le, F., Hao, Q., Sun, J., Liu, C. and Cai, Y.: Nutrient limitation of phytoplankton in anticyclonic eddies of the northern South China Sea, Biogeosciences Discuss., 5(6), 4591–4619, doi:10.5194/bgd-5-4591-2008, 2008.

Pan, X., Wong, G. T. F., Shiah, F. K. and Ho, T. Y.: Enhancement of biological productivity by internal waves: Observations in the summertime in the northern South China Sea, J. Oceanogr., 68(3), 427–437, doi:10.1007/s10872-012-0107-y, 2012.

Parsons, T. R., Maita, Y. and Lalli, C. M.: A Manual of Chemical & Biological Methods for Seawater Analysis, Pergamon Press, Oxford, UK., 1984.

Quay, P. D., Peacock, C., Bjrkman, K. and Karl, D. M.: Measuring primary production rates in the ocean: Enigmatic results between incubation and non-incubation methods at Station ALOHA, Global Biogeochem. Cycles, 24(3), doi:10.1029/2009GB003665, 2010.

Rehder, G. and Suess, E.: Methane and pCO_2 in the Kuroshio and the South China Sea during maximum summer surface temperatures, Mar. Chem., 75(1–2), 89–108, doi:10.1016/S0304-4203(01)00026-3, 2001.

Reuer, M. K., Barnett, B. A., Bender, M. L., Falkowski, P. G. and Hendricks, M. B.: New estimates of Southern Ocean biological production rates from O_2/Ar ratios and the triple isotope composition of O_2, Deep Sea Res. Part I Oceanogr. Res. Pap., 54(6), 951–974, doi:10.1016/j.dsr.2007.02.007, 2007.

Shadwick, E. H., Tilbrook, B., Cassar, N., Trull, T. W. and Rintoul, S. R.: Summertime physical and biological controls on O_2 and CO_2 in the Australian Sector of the Southern Ocean, J. Mar. Syst., 147, 21–28, doi:10.1016/j.jmarsys.2013.12.008, 2015.

Shi, X., Li, H., Han, X., Wang, L. and Zhu, C.: Influence of typical mesoscale oceanographical process on the distribution of nutrients and dissolved oxygen in the Northern part of South China Sea in summer (in Chinese), Acta Sci. Circumstantiae, 34(3), 695–703, doi:10.13671/j.hjkxxb.2014.0121, 2014.

Stanley, R. H. R., Kirkpatrick, J. B., Cassar, N., Barnett, B. A. and Bender, M. L.: Net community production and gross primary production rates in the western equatorial Pacific, Global Biogeochem. Cycles, 24(4), doi:10.1029/2009GB003651, 2010.

Su, J. and Yuan, Y.: Coastal hydrology of China (in Chinese), China Ocean Press, Beijing, China., 2005.

Takahashi, T., Sutherland, S. C., Wanninkhof, R., Sweeney, C., Feely, R. A., Chipman, D. W., Hales, B., Friederich, G., Chavez, F., Sabine, C., Watson, A., Bakker, D. C. E., Schuster, U., Metzl, N., Yoshikawa-Inoue, H., Ishii, M., Midorikawa, T., Nojiri, Y., Körtzinger, A., Steinhoff, T., Hoppema, M., Olafsson, J., Arnarson, T. S., Tilbrook, B., Johannessen, T., Olsen, A., Bellerby, R., Wong, C. S., Delille, B., Bates, N. R. and de Baar, H. J. W.: Climatological mean and decadal change in surface ocean pCO_2, and net sea–air CO_2 flux over the global oceans, Deep Sea Res. Part II Top. Stud. Oceanogr., 56(8–10), 554–577, doi:10.1016/j.dsr2.2008.12.009, 2009.

Tamminen, T.: Effects of ammonium effluents on planktonic primary production and decomposition in a coastal brackish water environment I. Nutrient balance of the water body and effluent tests, Netherlands J. Sea Res., 16(C), 455–464, doi:10.1016/0077-7579(82)90050-3, 1982.

Teeter, L., Hamme, R. C., Ianson, D. and Bianucci, L.: Accurate Estimation of Net Community Production From O_2/Ar Measurements, Global Biogeochem. Cycles, 32(8), 1163–1181, doi:10.1029/2017GB005874, 2018.

Teira, E., Mouriño, B., Marañón, E., Pérez, V., Pazó, M. J., Serret, P., De Armas, D., Escánez, J., Woodward, E. M. S. and Fernández, E.: Variability of chlorophyll and primary production in the Eastern North Atlantic Subtropical Gyre: Potential factors affecting phytoplankton activity, Deep. Res. Part I Oceanogr. Res. Pap., 52(4), 569–588, doi:10.1016/j.dsr.2004.11.007, 2005.

Tortell, P. D.: Dissolved gas measurements in oceanic waters made by membrane inlet mass spectrometry, Limnol. Oceanogr. Methods, 3(1), 24–37, doi:10.4319/lom.2005.3.24, 2005.

Tortell, P. D., Asher, E. C., Ducklow, H. W., Goldman, J. A. L., Dacey, J. W. H., Grzymski, J. J., Young, J. N., Kranz, S. A., Bernard, K. S. and Morel, F. M. M.: Metabolic balance of coastal Antarctic waters revealed by autonomous pCO_2 and ΔO_2/Ar measurements, Geophys. Res. Lett., 41(19), 6803–6810, doi:10.1002/2014GL061266, 2014.

Tortell, P. D., Merzouk, A., Ianson, D., Pawlowicz, R. and Yelland, D. R.: Influence of regional climate forcing on surface water pCO_2, ΔO_2/Ar and dimethylsulfide (DMS) along the southern British Columbia coast, Cont. Shelf Res., 47, 119–132, doi:10.1016/j.csr.2012.07.007, 2012.

Ulfsbo, A., Cassar, N., Korhonen, M., Van Heuven, S., Hoppema, M., Kattner, G. and Anderson, L. G.: Late summer net community production in the central Arctic Ocean using multiple approaches, Global Biogeochem. Cycles, 28(10), 1129–1148, doi:10.1002/2014GB004833, 2014.

Uu, D. V. and Brankart, J. M.: Seasonal variation of temperature and salinity fields and water masses in the Bien Dong (South China) Sea, Math. Comput. Model., 26(12), 97–113, doi:10.1016/S0895-7177(97)00243-4, 1997.

Wang, N., Lin, W., Cheng, B. and Huang, B.: Metabolic states of the Taiwan Strait and the northern South China Sea in summer 2012 (in Chinese), J. Trop. Oceanogr., 33(4), 61–68, doi:10.3969/j.issn.1009-5470.2014.04.008, 2014.

Wanninkhof, R.: Relationship between wind speed and gas exchange over the ocean, J. Geophys. Res. Oceans, 97(C5), 7373–7382, doi:10.1029/92JC00188, 1992.

Weiss, R. F.: The solubility of nitrogen, oxygen and argon in water and seawater, Deep Sea Res. Oceanogr. Abstr., 17(4), 721–735, doi:10.1016/0011-7471(70)90037-9, 1970.

Zhai, W., Dai, M. and Cai, W.: Coupling of surface pCO_2 and dissolved oxygen in the northern South China Sea: Impacts of contrasting coastal processes, Biogeosciences, 6(11), 2589–2598, doi:10.5194/bg-6-2589-2009, 2009.

Zhang, R., Zhu, X., Yang, C., Ye, L., Zhang, G., Ren, J., Wu, Y., Liu, S., Zhang, J. and Zhou, M.: Distribution of dissolved iron in the Pearl River (Zhujiang) Estuary and the northern continental slope of the South China Sea, Deep. Res. Part II Top. Stud. Oceanogr., 167, 14–24, doi:10.1016/j.dsr2.2018.12.006, 2019.

Table Captions:

Table 1. Basic information at all CTD stations in October 2014

Table 2. Basic information at all CTD stations in June 2015

Table 3. The start date and duration (Δday) of shelf water intrusion at stations with surface salinity lower than 33 in June 2015

Table4. Satellite-PAR data and NCP at selected stations in October 2014

Figure Captions:

Figure 1. Cruise tracks of two cruises in the slope region of the Northern South China Sea in **(a)** October 2014, **(b)** June 2015. The sea level height anomaly (SLA) and geostrophic current during observations in June 2015 (Chen et al., 2016) are shown in **(c)**. The black dots/stars represent the locations of the CTD casts. Red numbers indicate transects, while black numbers indicate the serial number of CTD stations based on the cruise plan. The color scale in **(a)** and **(b)** represents bathymetry.

Figure 2. Surface distributions of **(a)** temperature, **(b)** salinity, **(c)** chlorophyll-a (Chl a), and **(d)** $\Delta(O_2/Ar)$ in October 2014

Figure 3. Surface distributions of **(a)** temperature, **(b)** salinity, **(c)** chlorophyll-a (Chl a), **(d)** dissolved oxygen (DO), **(e)** pCO_2, and **(f)** $\Delta(O_2/Ar)$ in June 2015

Figure 4. Surface distribution of NCP among the northern slope of SCS during the cruise in **(a)** October 2014 and **(b)** June 2015.

Figure 5. Zonal variations in **(a)** temperature, salinity, **(b)** $\Delta(O_2/Ar)$, **(c)** Chl a, NCP and surface concentration of ammonia (NH_4^+) along Transect 5 in October 2014. The plots of $\Delta(O_2/Ar)$ and NCP are 10-point Savitzky-Golay smoothed to give a better view of their distribution.

Figure 6. Meridional variations in **(a)** temperature, salinity, **(b)** $\Delta(O_2/Ar)$, pCO_2, **(c)** Chl a, NCP and surface concentration of DIN along Transect 4 in June 2015. The plots of $\Delta(O_2/Ar)$, pCO_2 and NCP are 10-point Savitzky-Golay smoothed.

Figure 7. Principal Component Analysis (PCA) among variables for **(a)** October 2014 and **(b)** June 2015 (Bartlett's test of sphericity: $p < 0.01$)

Figure 8. **(a)** T-S diagram of surface DIN concentration in June 2015. The stations influenced by shelf water were in the red circle. **(b)** Correlation analysis between surface DIN concentration and NCP at sampling stations. The stations (characterized with $S < 33$) influenced by shelf water presented surface DIN concentration ≥ 0.27 μmol L^{-1}.

Figure 9. Correlation analysis between underway NCP and physical parameters (temperature and salinity) in October 2014 **(a, b)** and June 2015 **(c, d)**.

Table 1. Basic information at all CTD stations in October 2014

Station	Date of observation[a]	MLD (m)	Z_{eu}[b] (m)	k[c] ($m\ d^{-1}$)	τ[d] (d)
O-01	2014/10/13	58	82	4.7	12
O-02	2014/10/13	64	74	5.2	12
O-03	2014/10/14	56	84	6.2	9
O-04	2014/10/14	54	76	6.3	9
O-05	2014/10/20	27	70	7.9	3
O-06	2014/10/19	55	62	8.4	7
O-07	2014/10/21	40	60	7.3	5
O-08	2014/10/21	49	72	7.4	7
O-09	2014/10/15	79	96	6.2	13
O-10	2014/10/15	68	81	6.1	11
O-11	2014/10/15	64	81	5.4	12
O-12	2014/10/16	66	74	5.2	13
O-13	2014/10/16	48	52	6.3	8
O-14	2014/10/17	54	62	6.9	8
O-15	2014/10/22	49	68	7.0	7
O-16	2014/10/22	50	73	7.3	7
O-17	2014/10/23	52	75	7.9	7
O-19	2014/10/18	31	64	9.4	3
O-20	2014/10/18	35	61	8.7	4
O-21	2014/10/18	81	86	6.9	12
O-22	2014/10/17	76	102	6.0	13

[a] All dates are in the format of year/month/day. [b] Euphotic depth, defined based on subsurface chlorophyll maximum layer. [c] Gas transfer velocity of O_2. [d] Residence time of O_2 in the mixed layer, estimated as per MLD/k.

Table 2. Basic information at all CTD stations in June 2015

Station	**Date of observation**	**MLD (m)**	**Z_{eu} (m)**	**k (m d^{-1})**	**τ (d)**
J-01	2015/6/18	26	63	2.2	12
J-02	2015/6/17	19	80	1.9	10
J-03	2015/6/16	20	74	1.9	11
J-04	2015/6/15	22	74	1.9	11
J-05	2015/6/15	11	78	1.2	9
J-06	2015/6/14	24	76	2.1	11
J-07	2015/6/13	21	81	2.3	9
J-08	2015/6/18	14	56	1.7	8
J-09	2015/6/19	17	59	1.6	10
J-10	2015/6/19	8	46	1.4	6
J-11	2015/6/20	8	40	2.8	3
J-12	2015/6/21	16	45	3.0	5
J-13	2015/6/21	19	45	2.3	8
J-14	2015/6/24	28	55	4.0	7
J-15	2015/6/24	17	42	5.3	3
J-16	2015/6/25	10	19	5.7	2

Table 3. The start date and duration (Δday) of shelf water intrusion at stations with surface salinity lower than 33 in June 2015

Station	**Date of observation**	**Start date of shelf water intrusion**	**Δday[a]**	**τ (d)**
J-09	2015/6/19	2015/6/10	9	10
J-10	2015/6/19	2015/6/13	6	6
J-11	2015/6/20	2015/6/13	7	3
J-12	2015/6/21	2015/6/13	8	5
J-13	2015/6/21	2015/6/13	8	8
J-16	2015/6/25	before 2015/6/10	> 15	2

[a] The difference between the date of observation and the start date of shelf water intrusion at listed stations.

Table 4. Satellite-PAR data and NCP at selected stations in October 2014

Station	Date of observation	MLD (m)	Z_{eu} (m)	Surface PAR[a] (mol m^{-2} d^{-1})	K_d (m^{-1})	ML PAR[b] (mol m^{-2} d^{-1})	NCP (mmol C m^{-2} d^{-1})
O-01	2014/10/13	58	82	42.0	$5.6 * 10^{-2}$	12.0	3.0
O-02	2014/10/13	64	74	42.0	$6.2 * 10^{-2}$	10.0	15.1
O-03	2014/10/14	56	84	41.1	$5.5 * 10^{-2}$	12.4	10.1
O-08	2014/10/21	49	72	38.7	$6.4 * 10^{-2}$	11.4	15.7
O-10	2014/10/15	68	81	40.0	$5.7 * 10^{-2}$	9.8	4.4
O-13	2014/10/16	48	52	39.2	$8.9 * 10^{-2}$	8.7	15.3
O-15	2014/10/22	49	68	38.6	$6.8 * 10^{-2}$	10.8	16.3
O-20	2014/10/18	35	61	39.2	$7.5 * 10^{-2}$	13.3	16.4
O-22	2014/10/17	76	102	42.2	$4.5 * 10^{-2}$	11.6	15.7

[a] Average surface PAR over the residence time of O_2 in the mixed layer. [b] Average PAR in the mixed layer.

861

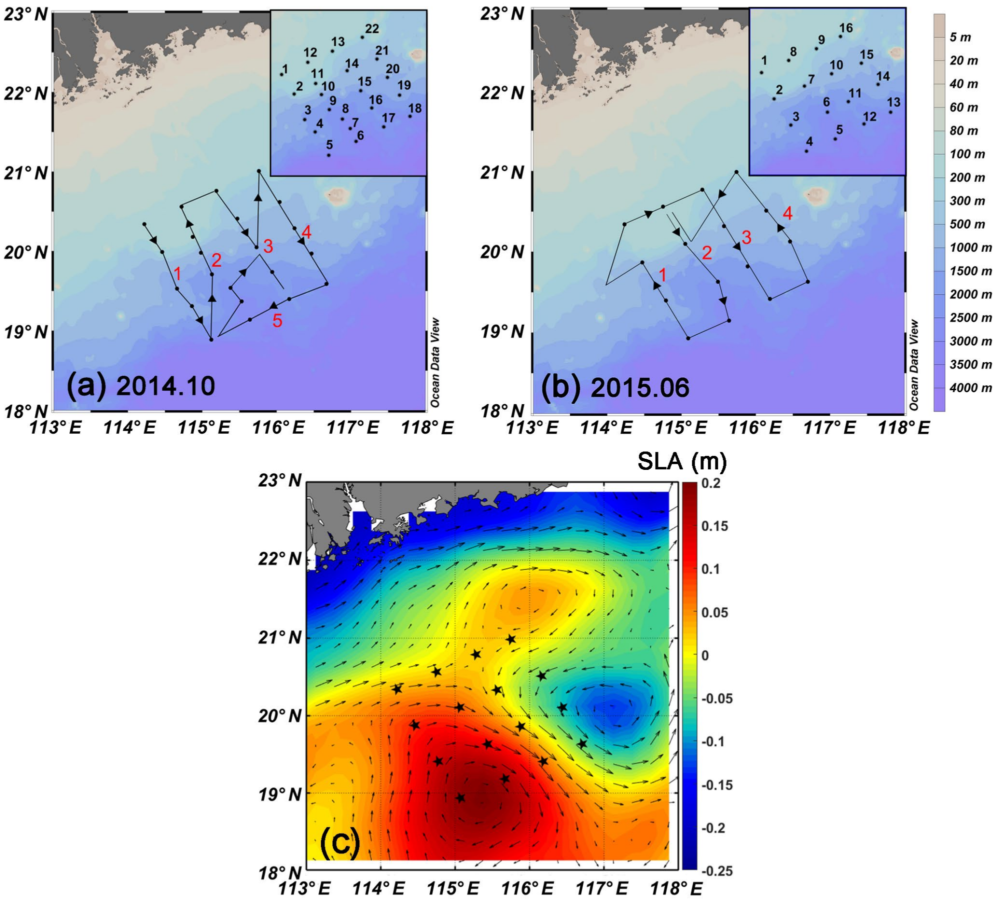

Figure 1. Cruise tracks of two cruises in the slope region of the Northern South China Sea in **(a)** October 2014, **(b)** June 2015. The sea level height anomaly (SLA) and geostrophic current during observations in June 2015 (Chen et al., 2016) are shown in **(c)**. The black dots/stars represent the locations of the CTD casts. Red numbers indicate transects, while black numbers indicate the serial number of CTD stations based on the cruise plan. The color scale in **(a)** and **(b)** represents bathymetry.

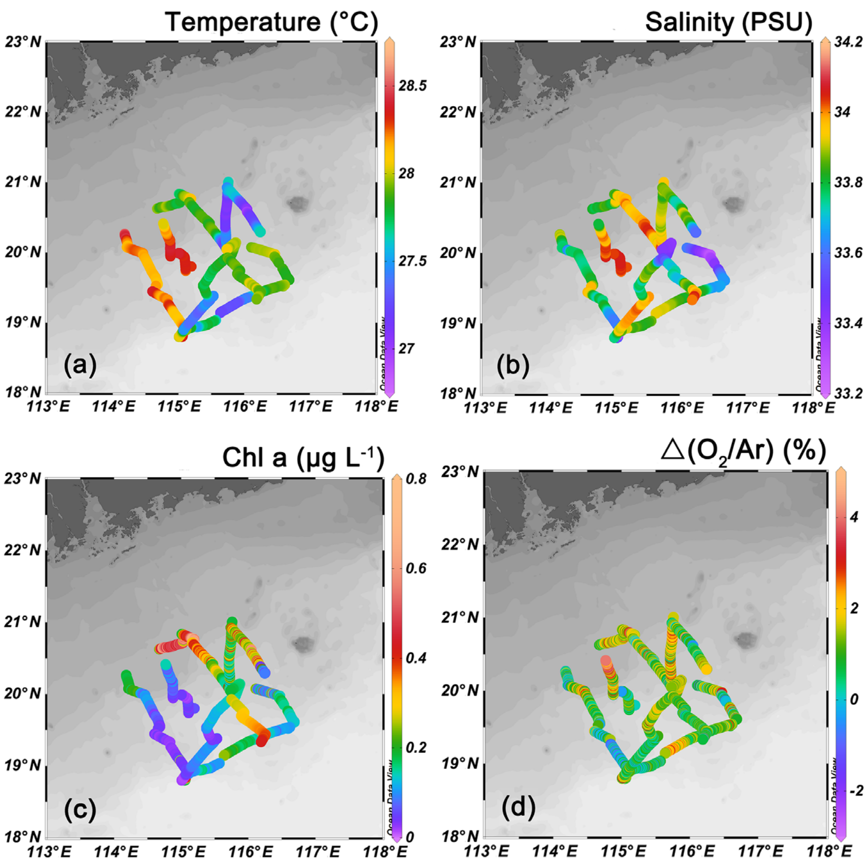

Figure 2. Surface distributions of **(a)** temperature, **(b)** salinity, **(c)** chlorophyll-a (Chl a), and **(d)** $\Delta(O_2/Ar)$ in October 2014

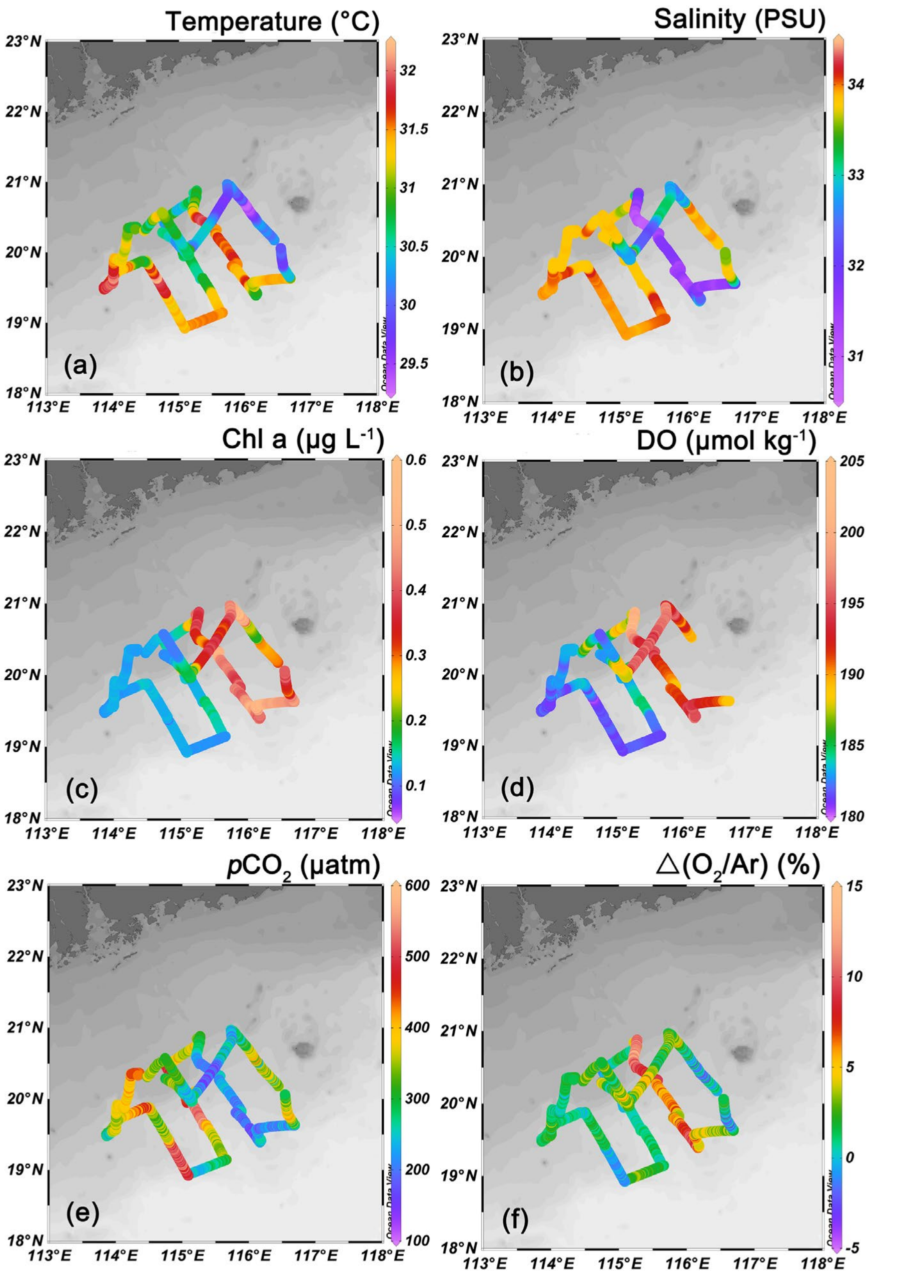

Figure 3. Surface distributions of **(a)** temperature, **(b)** salinity, **(c)** chlorophyll-a (Chl a), **(d)** dissolved oxygen (DO), **(e)** pCO_2, and **(f)** $\Delta(O_2/Ar)$ in June 2015

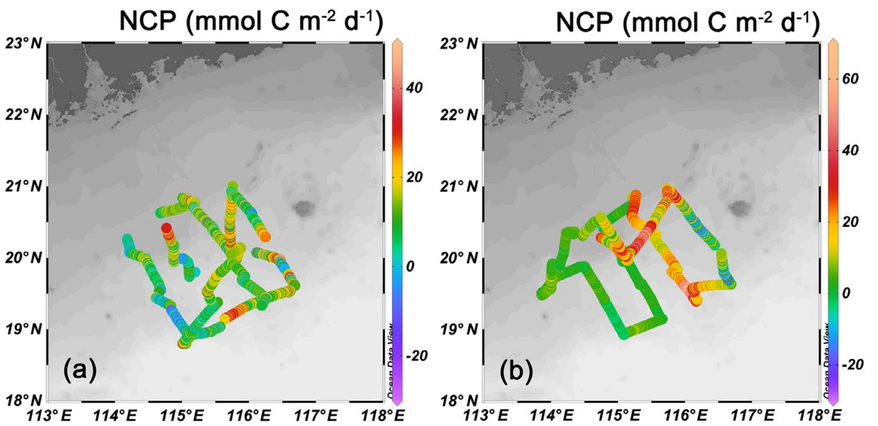

Figure 4. Surface distribution of NCP among the northern slope of SCS during the cruise in **(a)** October 2014 and **(b)** June 2015.

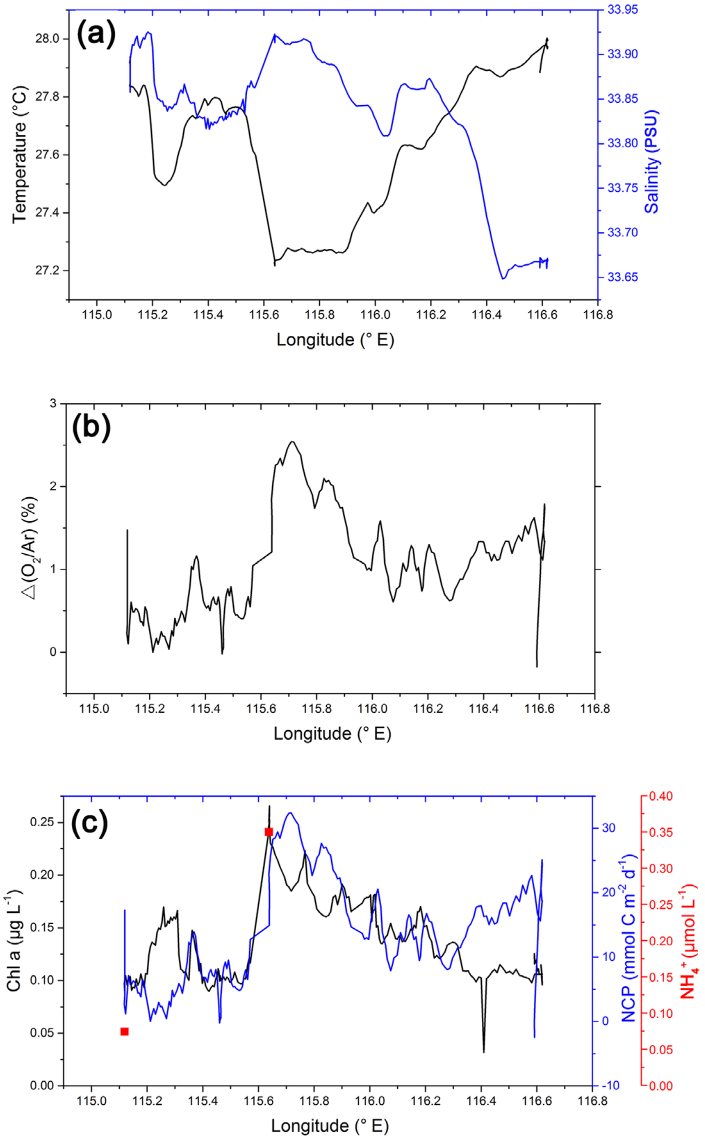

Figure 5. Zonal variations in **(a)** temperature, salinity, **(b)** $\Delta(O_2/Ar)$, **(c)** Chl a, NCP and surface concentration of ammonia (NH_4^+) along Transect 5 in October 2014. The plots of $\Delta(O_2/Ar)$ and NCP are 10-point Savitzky-Golay smoothed to give a better view of their distribution.

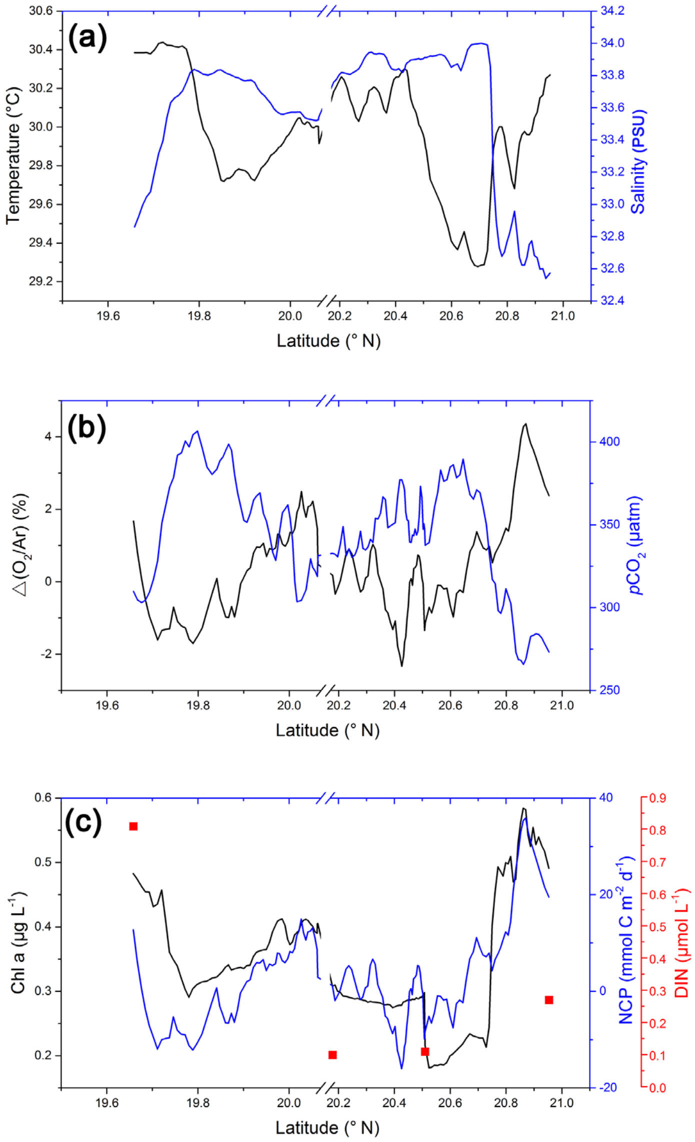

Figure 6. Meridional variations in **(a)** temperature, salinity, **(b)** $\Delta(O_2/Ar)$, pCO_2, **(c)** Chl a, NCP and surface concentration of DIN along Transect 4 in June 2015. The plots of $\Delta(O_2/Ar)$, pCO_2 and NCP are 10-point Savitzky-Golay smoothed.

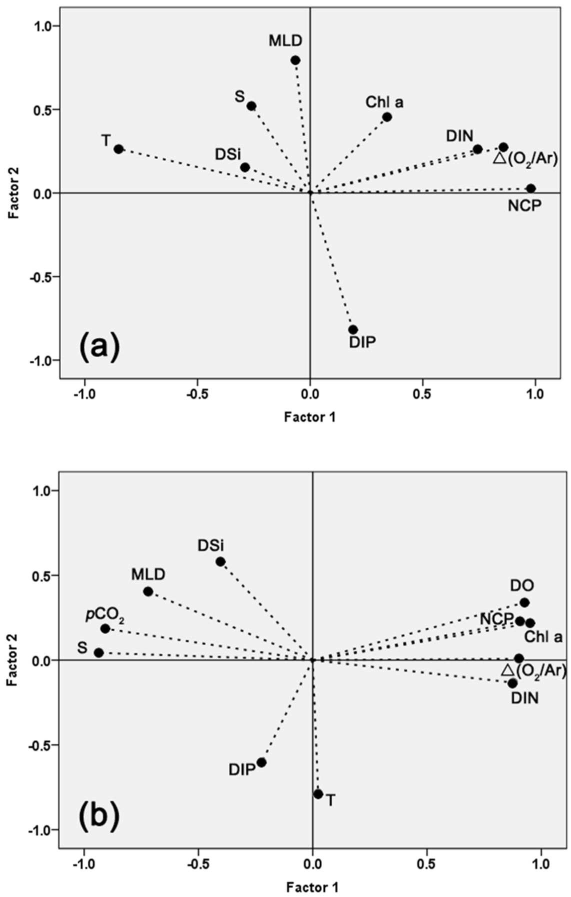

Figure 7. Principal Component Analysis (PCA) among variables for **(a)** October 2014 and **(b)** June 2015 (Bartlett's test of sphericity: $p < 0.01$)

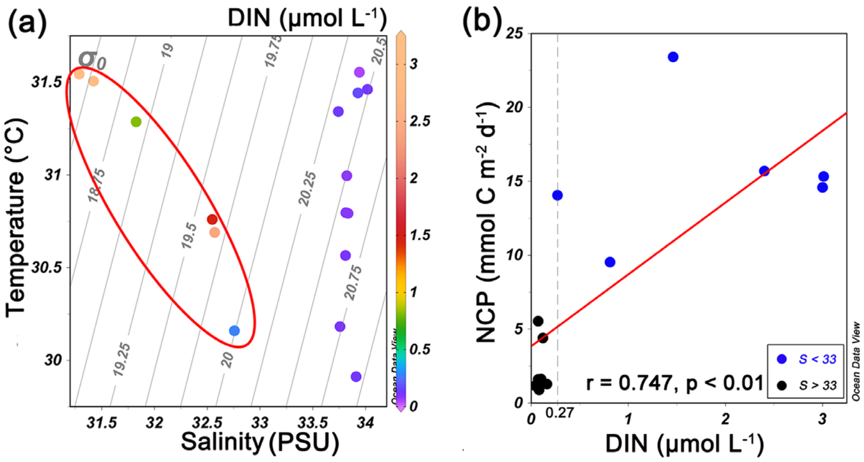

Figure 8. **(a)** T-S diagram of surface DIN concentration in June 2015. The stations influenced by shelf water were in the red circle. **(b)** Correlation analysis between surface DIN concentration and NCP at sampling stations. The stations (characterized with $S < 33$) influenced by shelf water presented surface DIN concentration ≥ 0.27 μmol L^{-1}.

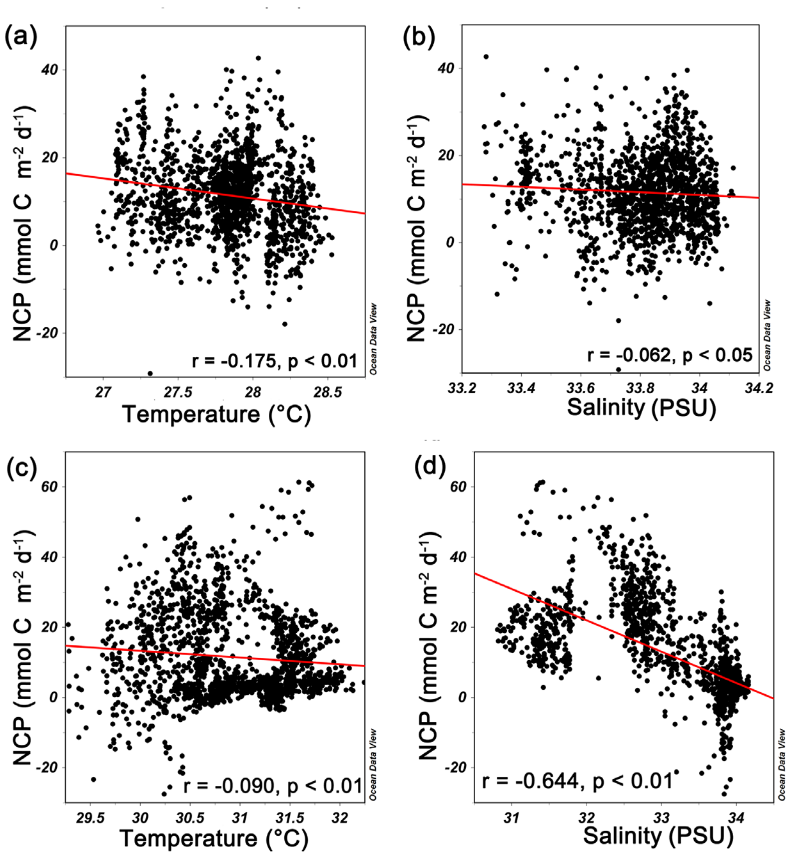

Figure 9. Correlation analysis between underway NCP and physical parameters (temperature and salinity) in October 2014 **(a, b)** and June 2015 **(c, d)**.

Supplementary

Table S1a. Correlation coefficient matrix of PCA in October 2014

		Temperature (T)	Salinity (S)	DIN	DIP	DSi	MLD	Chl a	$\Delta(O_2/Ar)$	NCP
Correlation coefficient	Temperature (T)	1.000	0.190	−0.536	−0.305	0.539	0.267	−0.162	−0.524	−0.757
	Salinity (S)	0.190	1.000	0.098	−0.337	−0.492	0.352	0.145	−0.295	−0.359
	DIN	−0.536	0.098	1.000	0.000	−0.132	0.176	0.125	0.574	0.706
	DIP	−0.305	−0.337	0.000	1.000	−0.264	−0.494	−0.267	−0.075	0.135
	DSi	0.539	−0.492	−0.132	−0.264	1.000	0.098	0.051	−0.024	−0.171
	MLD	0.267	0.352	0.176	−0.494	0.098	1.000	0.068	0.202	−0.037
	Chl a	−0.162	0.145	0.125	−0.267	0.051	0.068	1.000	0.397	0.323
	$\Delta(O_2/Ar)$	−0.524	−0.295	0.574	−0.075	−0.024	0.202	0.397	1.000	0.906
	NCP	−0.757	−0.359	0.706	0.135	−0.171	−0.037	0.323	0.906	1.000
Statistical significance	Temperature (T)		0.288	0.044	0.181	0.043	0.214	0.317	0.049	0.003
	Salinity (S)	0.288		0.388	0.155	0.062	0.144	0.335	0.189	0.139
	DIN	0.044	0.388		0.500	0.350	0.302	0.358	0.032	0.008
	DIP	0.181	0.155	0.500		0.216	0.061	0.214	0.413	0.346
	DSi	0.043	0.062	0.350	0.216		0.387	0.441	0.473	0.307
	MLD	0.214	0.144	0.302	0.061	0.387		0.422	0.275	0.457
	Chl a	0.317	0.335	0.358	0.214	0.441	0.422		0.113	0.167
	$\Delta(O_2/Ar)$	0.049	0.189	0.032	0.413	0.473	0.275	0.113		0.000
	NCP	0.003	0.139	0.008	0.346	0.307	0.457	0.167	0.000	

Table S1b. Component matrix of variables in October 2014

	Factor 1	Factor 2
Temperature (T)	−0.847	0.264
Salinity (S)	−0.259	0.521
DIN	0.741	0.259
DIP	0.189	−0.817
DSi	−0.288	0.156
MLD	−0.065	0.793
Chl a	0.343	0.456
$\Delta(O_2/Ar)$	0.858	0.276
NCP	0.979	0.026

Table S2a. Correlation coefficient matrix of PCA in June 2015

		Temperature (T)	Salinity (S)	DIN	DIP	DSi	MLD	Chl a	pCO_2	DO	$\Delta(O_2/Ar)$	NCP
Correlation coefficient	Temperature (T)	1.000	−0.128	0.217	0.150	−0.239	−0.244	−0.156	−0.189	−0.313	0.060	−0.224
	Salinity (S)	−0.128	1.000	−0.873	0.163	0.301	0.614	−0.921	0.859	−0.831	−0.816	−0.787
	DIN	0.217	−0.873	1.000	−0.067	−0.260	−0.594	0.754	−0.705	0.736	0.910	0.747
	DIP	0.150	0.163	−0.067	1.000	−0.222	−0.017	−0.349	0.165	−0.355	−0.172	−0.195
	DSi	−0.239	0.301	−0.260	−0.222	1.000	0.474	−0.275	0.443	−0.241	−0.361	−0.276
	MLD	−0.244	0.614	−0.594	−0.017	0.474	1.000	−0.593	0.816	−0.541	−0.507	−0.518
	Chl a	−0.156	−0.912	0.754	−0.349	−0.275	−0.593	1.000	−0.867	0.948	0.793	0.884
	pCO_2	−0.189	0.859	−0.705	0.165	0.443	0.816	−0.867	1.000	−0.762	−0.701	−0.767
	DO	−0.313	−0.831	0.736	−0.355	−0.241	−0.541	0.948	−0.762	1.000	0.839	0.946
	$\Delta(O_2/Ar)$	0.060	−0.816	0.910	−0.172	−0.361	−0.507	0.793	−0.701	0.839	1.000	0.846
	NCP	−0.224	−0.787	0.747	−0.195	−0.276	−0.518	0.884	−0.767	0.946	0.846	1.000
Statistical significance	Temperature (T)		0.331	0.228	0.305	0.205	0.200	0.297	0.259	0.138	0.420	0.220
	Salinity (S)	0.331		0.000	0.288	0.148	0.010	0.000	0.000	0.000	0.000	0.000
	DIN	0.228	0.000		0.410	0.185	0.013	0.001	0.002	0.001	0.000	0.001
	DIP	0.305	0.288	0.410		0.223	0.477	0.111	0.286	0.106	0.279	0.252
	DSi	0.205	0.148	0.185	0.223		0.043	0.170	0.056	0.203	0.102	0.170
	MLD	0.200	0.010	0.013	0.477	0.043		0.013	0.000	0.023	0.032	0.029
	Chl a	0.297	0.000	0.001	0.111	0.170	0.013		0.000	0.000	0.000	0.000
	pCO_2	0.259	0.000	0.002	0.286	0.056	0.000	0.000		0.001	0.003	0.001
	DO	0.138	0.000	0.001	0.106	0.203	0.023	0.000	0.001		0.000	0.000
	$\Delta(O_2/Ar)$	0.420	0.000	0.000	0.279	0.102	0.032	0.000	0.003	0.000		0.000
	NCP	0.220	0.000	0.001	0.252	0.170	0.029	0.000	0.001	0.000	0.000	

916

Table S2b. Component matrix of variables in June 2015

	Factor 1	Factor 2
Temperature (T)	0.024	−0.786
Salinity (S)	−0.936	0.043
DIN	0.876	−0.132
DIP	−0.223	−0.601
DSi	−0.405	0.582
MLD	−0.718	0.402
Chl a	0.950	0.217
pCO_2	−0.908	0.186
DO	0.927	0.340
$\Delta(O_2/Ar)$	0.902	0.008
NCP	0.909	0.227

917

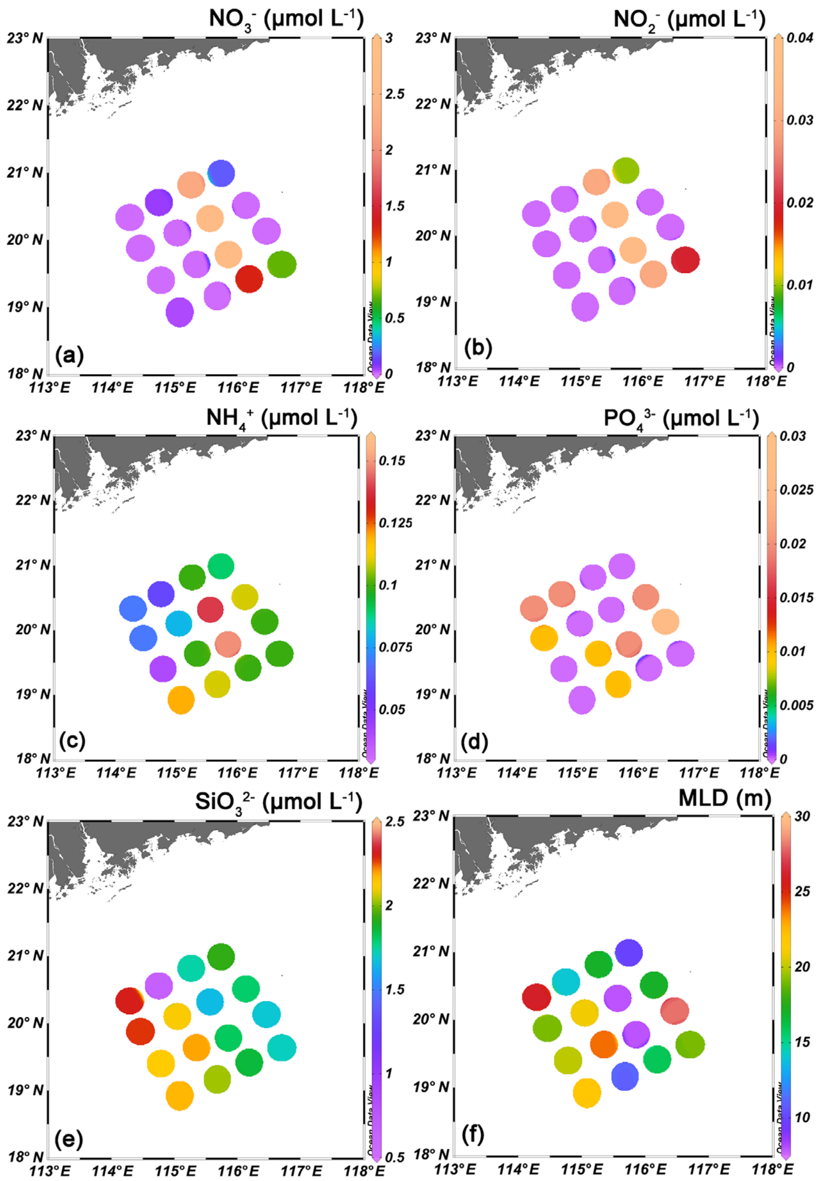

Figure S1. Surface distributions of **(a)** nitrate (NO_3^-), **(b)** nitrite (NO_2^-), **(c)** ammonium (NH_4^+), **(d)** phosphate (PO_4^{3-}), **(e)** silicate (SiO_3^{2-}) and **(f)** mixed layer depth (MLD) in June 2015. We regarded the nutrients data that were below the detection limit as "0" when made these plots.

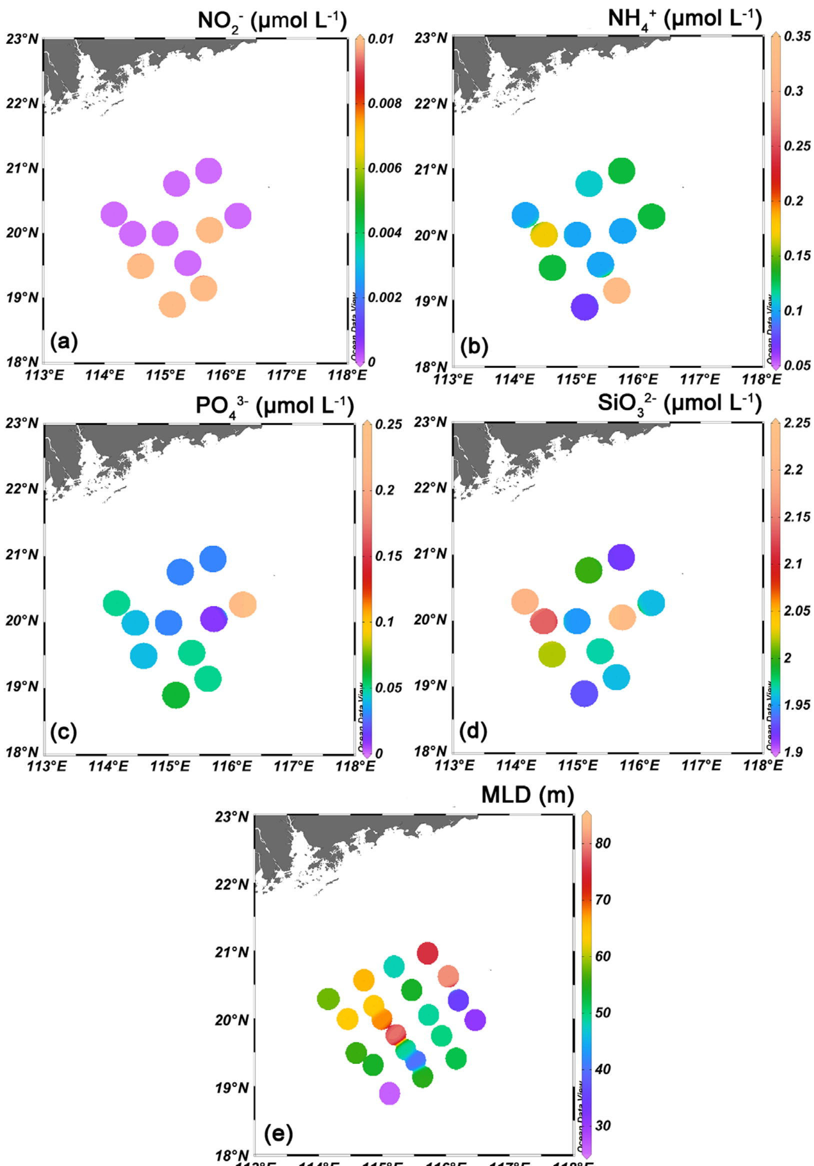

Figure S2. Surface distributions of **(a)** nitrite (NO_2^-), **(b)** ammonium (NH_4^+), **(c)** phosphate (PO_4^{3-}), **(d)** silicate (SiO_3^{2-}) and **(e)** mixed layer depth (MLD) in October 2014. The surface concentration of nitrate (NO_3^-) at all sampling stations was below the detection limit during this cruise. We regarded the nutrients data that were below the detection limit as "0" when made these plots.

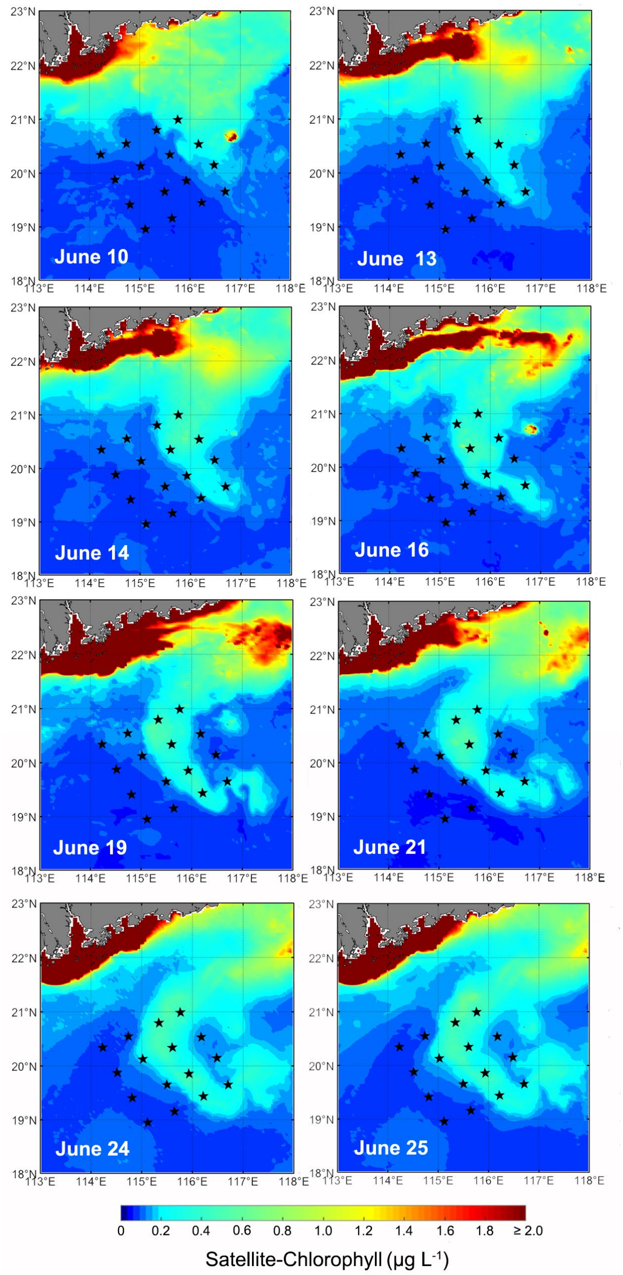

Figure S3. Daily satellite-chlorophyll on selected date from June 10 to 25, 2015. Stars represent CTD locations. We roughly set light blue (represents ~ 0.2 μg L^{-1}) in this figure as the criterion of shelf water. This figure was made based on the M_Map mapping package for MATLAB (Pawlowicz, R., 2020. "M_Map: A mapping package for MATLAB", version 1.4m, [Computer software], available online at www.eoas.ubc.ca/~rich/map.html.).